

# CHEMICAL ENGINEERING SCIENCE

## GENIE CHIMIQUE

VOL. 2

FEBRUARY 1953

NO. 1

### Continuous flow systems

#### Distribution of Residence Times

P. V. DANCKWERTS

Department of Chemical Engineering, Tennis Court Road, Cambridge, England

(Received 24 October 1952)

**Summary**—When a fluid flows through a vessel at a constant rate, either "piston-flow" or perfect mixing is usually assumed. In practice many systems do not conform to either of these assumptions, so that calculations based on them may be inaccurate. It is explained how distribution-functions for residence-times can be defined and measured for actual systems. Open and packed tubes are discussed as systems about which predictions can be made. The use of the distribution-functions is illustrated by showing how they can be used to calculate the efficiencies of reactors and blenders. It is shown how models may be used to predict the distribution of residence-times in large systems.

**Résumé**—Quand, dans un récipient, on introduit, à vitesse constante, un fluide donné, on suppose généralement soit un mélange parfait, soit un "écoulement frontal parfait." En pratique, de nombreux systèmes s'écartent de l'une ou l'autre de ces hypothèses simplificatrices et les calculs qui en résultent sont plus ou moins inexacts. L'auteur expose, pour des systèmes réels, comment l'on peut définir et mesurer des fonctions de distribution pour la "durée de séjour": ceci peut s'appliquer à des tubes vides ou munis de garnissages. Par emploi de ces fonctions de distribution, l'auteur montre comment on peut calculer l'efficacité des réacteurs ou des mélangeurs. Des modèles peuvent être utilisés pour prévoir la répartition des "durées de séjour" dans des systèmes de grandes dimensions.

When a stream of material flows steadily through a vessel such as a pipe or a tank, in which it takes part in some process such as chemical reaction, heat- or mass-transfer, or simple mixing, it is usual to make use of one of the following assumptions for the purposes of calculation:

(a) The fluid in the vessel is completely mixed, so that its properties are uniform and identical with those of the outgoing stream. This assumption is frequently made the basis of calculations on stirred reactors or blenders.

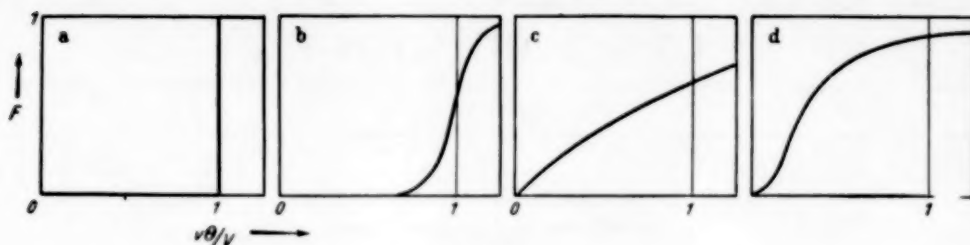
(b) Elements of fluid which enter the vessel at the same moment move through it with constant and equal velocity on parallel paths, and leave at the same moment. This type of behaviour will be referred to as "piston flow," and is normally assumed when considering flow through heat-exchangers, catalytic reactors, packed towers, chromatographic columns, etc.

It is clear that there are many cases in which neither type of flow corresponds exactly to the facts—for instance, fluid in laminar flow in a pipe, or gas

flowing through a fluidised catalytic reactor or blast furnace. It is of some importance to investigate the discrepancies between the assumed and actual behaviour of such systems, and where necessary to allow for them in making calculations. This paper is intended to clarify some of the problems presented by steady-flow systems, and to show how their behaviour can be investigated and quantitatively specified. Some of the concepts and mathematical expressions which appear below have already been used by GILLILAND and MASON [8], [9] in the course of a study of flow through fluidised beds.

#### *F*-DIAGRAMS AND AGE-DISTRIBUTION FUNCTIONS

The volume of the vessel occupied by the fluid is  $V$ , and the volumetric rate of inflow and outflow of fluid is assumed constant and equal to  $v$ . Suppose some property of the inflowing fluid undergoes a sudden change from one steady value to another; for instance, let the colour change from white to red. Call the fraction of red material in the outflow at time  $\theta$  later be  $F(\theta)$ . The plot of  $F(\theta)$  vs.  $v\theta/V$

Fig. 1. *F*-diagrams.

- (a) Piston flow; (b) Piston flow with some longitudinal mixing; (c) Complete mixing; (d) Dead water.

will be called an "*F*-diagram." Figs. 1 (a)-(d) show *F*-diagrams for some representative types of system.

Perfect piston flow (1(a)) will never occur with Newtonian fluids; there will always be some longitudinal mixing, due to viscous effects and molecular or eddy-diffusion. 1 (b) illustrates the departure from piston flow caused by restricted longitudinal mixing. 1 (c) is the diagram for perfect mixing; the equation of the curve is easily shown to be:

$$F(\theta) = 1 - e^{-v\theta/V}. \quad (1)$$

It cuts the ordinate  $v\theta/V = 1$  at  $(1 - \frac{1}{e})$ , and its initial slope is unity. 1 (d) shows a diagram of the type to be expected when there is a good deal of "dead water" in the system; a considerable fraction of the fluid is trapped in eddies, and spends much more than the average length of time in the vessel, while most of the flow takes place through a restricted channel.

The *F*-diagram of a system is easy to obtain (for instance, by injecting tracer materials into the entering stream), and its shape will clearly give a good deal of information about the behaviour of the fluid flowing through the vessel. As will be shown later, much of this information can be summarised by two numbers which can be derived from the *F*-diagram. The diagram also enables certain calculations to be made concerning the performance of the system when used, for instance, as a blender or reactor.

The shape of the *F*-diagram depends on the relative times taken by various portions of the fluid to flow through the vessel, or in other words, on the distribution of residence-times. Those elements of the material in the vessel which have been in it for a time  $\theta$  are said to have an "age"  $\theta$ , and the fraction

of the material in the system having at any instant ages between  $\theta$  and  $(\theta + d\theta)$  is  $I(\theta) d\theta$ . The fraction of the material having ages between  $\theta$  and  $(\theta + d\theta)$  at the moment of leaving the system is  $E(\theta) d\theta$ . *I* and *E* may be called the internal and exit age-distribution functions respectively. The relationship between *E*, *I* and *F* can be shown by imagining the ingoing stream, as before, to change from white to red at time  $\theta = 0$ . At a time  $\theta$  later the balance sheet for the red material is:

Entered:  $v\theta$ .

Still in system:  $V \int_0^\theta I(\theta') d\theta'$ .

Left system:  $v \int_{\theta'=0}^\theta \int_{\theta''=0}^{\theta'} E(\theta') d\theta' d\theta''$ .

(The last follows because the rate of outflow of red material at any time  $\theta''$  after the change of colour

is  $v \int_0^{\theta''} E(\theta') d\theta'$ ). Thus the conservation equation

for red material is

$$\frac{v\theta}{V} = \int_0^\theta I(\theta') d\theta' + \frac{v}{V} \int_{\theta'=0}^\theta \int_{\theta''=0}^{\theta'} E(\theta') d\theta' d\theta''. \quad (2)$$

Also, the total fraction  $F(\theta)$  of red material in the outflow at time  $\theta$  is

$$F(\theta) = \int_0^\theta E(\theta') d\theta'. \quad (3)$$

Differentiating (2) with respect to  $\theta$ :

$$1 - \int_0^\theta E(\theta') d\theta' = \frac{V}{v} I(\theta), \quad (4)$$

and hence from equation (3):

$$1 - F(\theta) = \frac{V}{v} I(\theta). \quad (5)$$

Equation (4) gives the relationship between  $E(\theta)$  and  $I(\theta)$ , while equation (5) shows how the latter function can be determined from the  $F$ -diagram.

The same information can be obtained in a somewhat different way, which may prove more convenient under some circumstances. Suppose a quantity  $Q$  of some substance (a radioactive tracer might be chosen for ease of estimation) is injected into the entering stream virtually instantaneously - that is, within a period very short compared to  $V/v$ . As

$$\frac{V}{Q} \int_0^\infty C(\theta) d\left(\frac{v\theta}{V}\right) = 1, \quad (7)$$

so that the area under every  $C$ -diagram is equal to unity.

It has been assumed in the foregoing that the forms of the functions  $I$  and  $E$  do not vary with time. In fact, however, instability of flow may lead to fluctuations in the internal and exit age-distributions, and cause observed values of  $F(\theta)$  to oscillate about some smooth curve of the kind shown in Fig. 1. These fluctuations will generally be random in nature, and by making a number of determinations of the  $F$ -diagram and averaging, the mean form of the diagram can be obtained. The problems raised by such fluctuations will be considered on another occasion; for the moment attention will be confined to cases where they may be ignored.

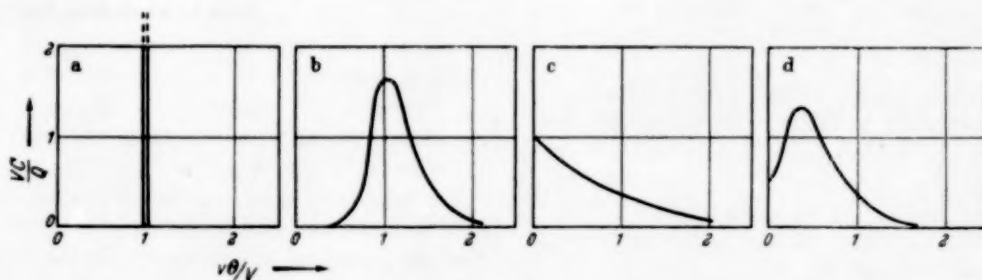


Fig. 2.  $C$ -diagrams.

(a) Piston flow

(b) Piston flow with some longitudinal mixing

(c) Complete mixing

(d) Dead water.

before, samples are taken at various times  $\theta$  after the injection; the concentration of the injected material in the exit stream at time  $\theta$  is  $C(\theta)$ . Then it can be shown, by methods similar to those used above, that

$$C(\theta) = \frac{Q}{v} \frac{d}{d\theta} \left\{ F(\theta) \right\} = \frac{Q}{v} E(\theta). \quad (6)$$

Plots of  $\frac{VC(\theta)}{Q}$  vs.  $\frac{v\theta}{V}$ , which may be called

$C$ -diagrams, are shown in Fig. 2 for the systems whose  $F$ -diagrams are given in Fig. 1. Note that

It will be noted that

$$\int_0^\infty I(\theta) d\theta \equiv \frac{v}{V} \int_0^\infty \left\{ 1 - F(\theta) \right\} d\theta = 1 \quad (8)$$

and

$$\int_0^\infty E(\theta) d\theta = 1 \quad (9)$$

(because the integrals in equations (8) and (9) represent the total fractions of material, in the vessel and at the exit respectively, having ages between

0 and  $\infty$  — namely, *all* the material in each case). Equation (8) implies that the area between the curve  $F(\theta)$  vs.  $v\theta/V$  and the line  $F(\theta) = 1$  is equal to unity. It can be seen immediately that the two shaded areas are equal in Fig. 3 whatever the shape of the curve.

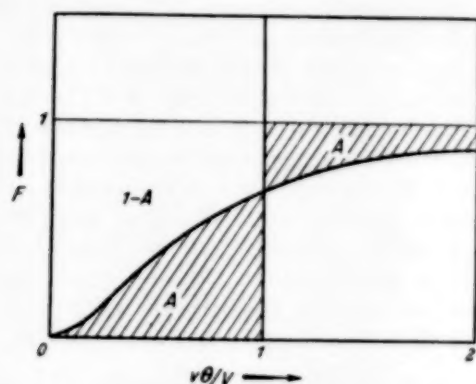


Fig. 3.

The average age  $\bar{\theta}_E$  of the material leaving the vessel is always  $V/v$ . This can be shown as follows:

$$\bar{\theta}_E = \int_0^{\infty} \theta \cdot E(\theta) d\theta. \quad (10)$$

Hence, from equation (3)

$$\frac{\bar{\theta}_E}{V} = \int_0^{\infty} \frac{v\theta}{V} \frac{dF(\theta)}{d\theta} d\theta = \int_{F=0}^1 \frac{v\theta}{V} dF(\theta). \quad (11)$$

It can be seen that from Fig. 3 that the last integral is equal to 1.

The average age of the material in the system at any time is  $\bar{\theta}_I$ , where

$$\bar{\theta}_I = \int_0^{\infty} \theta \cdot I(\theta) d\theta = \frac{v}{V} \int_0^{\infty} \theta \{1 - F(\theta)\} d\theta. \quad (12)$$

Integrating by parts we have

$$\bar{\theta}_I = \frac{v}{2V} \int_{F=0}^1 \theta^2 dF(\theta). \quad (13)$$

The integral in (12) or (13) can be evaluated graphically with the help of the  $F$ -diagram.

#### HOLD-BACK AND SEGREGATION

The systems illustrated in Figs. 1 (a)-(d) show in progressively greater degree a quality which will be called "hold-back." In a system which displays hold-back, some elements of fluid spend more, others less, than the average time,  $V/v$ , in the vessel. In a system with piston-flow (1 (a)), there is no hold-back. Quantitatively, the magnitude of the hold-back will be denoted by  $H$ , and can be conveniently defined as the area under the  $F$ -diagram between  $v\theta/V = 0$  and  $v\theta/V = 1$  (area  $A$  in Fig. 3):

$$H = \frac{v}{V} \int_0^{V/v} F(\theta) d\theta. \quad (14)$$

$H$  varies from 0 for piston-flow to values approaching 1 when most of the space in the vessel is dead water. For the completely mixed vessel (Fig. 1 (c)),  $H = 1/e$ . The magnitude of  $H$  is a measure of the deviation from piston-flow. Its significance is most easily visualised as follows: if the colour of the inflowing stream changes suddenly from white to red,  $H$  is equal to the fraction of the vessel which will still be occupied by white fluid after a volume of red fluid equal to the volume of the vessel has flowed in.

The hold-back is of importance in connection with chemical reactors and the successive flow of fluids through pipes and other vessels. In the former case it will usually be true to say that if the reactants are adequately mixed before or shortly after entering the vessel, the output of the reactor will be greatest when the hold-back is least (although the reverse may be true for autocatalytic reactions). A high hold-back means that much of the volume of the reactor is occupied by material which has already undergone reaction, while much reactant passes rapidly through the vessel by a "short-circuit" route. The magnitude of the hold-back gives only a general idea of the behaviour of the system, however; the whole  $F$ -diagram (and possibly other information) is needed if the actual performance of the reactor is to be calculated. This subject is discussed in a later section.

An indication of the efficiency of mixing in a system can be given by a single quantity,  $S$ , which will be called the "segregation," and can be derived from the  $F$ -diagram as follows. If one superimposes the



$F$ -diagrams for a perfectly-mixed system (equation (1)) and for an imperfectly mixed system such as that represented in Fig. 1 (b), the result will be similar to Fig. 4.

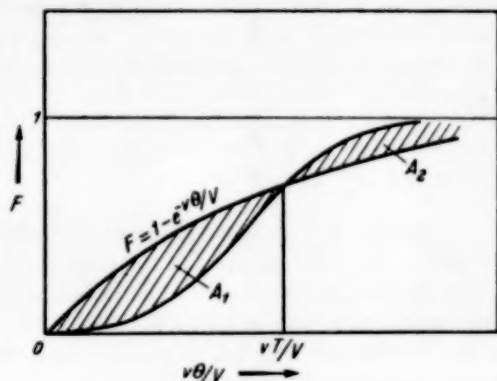


Fig. 4.

The degree of departure of the system from perfect mixing will be indicated by the size of the shaded area ( $A_1 + A_2$ ). However, since the area between each curve, and the line  $F(\theta) = 1$  is the same, the two shaded regions have the same area ( $A_1 = A_2$ ). It is thus convenient to define the segregation  $S$  quantitatively as the area  $A_1$  between the  $F$ -diagram of the system and the curve  $F(\theta) = 1 - e^{-\theta/V}$ , up to the point (at  $\theta = T$ ) where the curves cross; it is thus equal to half the total shaded area.

When there is dead water in the system the positions of the curves may be inverted, as in Fig. 5.

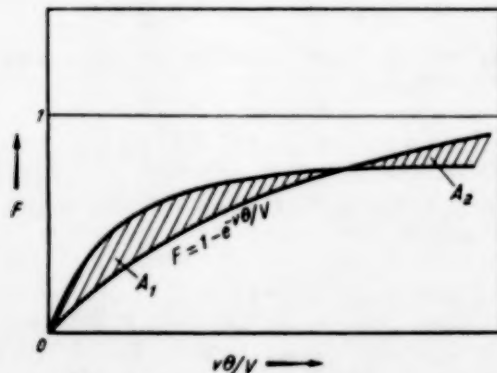


Fig. 5.

The segregation is then given the negative value  $-A_1$  to indicate the nature of the departure from perfect mixing. In a case such as that illustrated in Fig. 1 (b), the two curves may cut twice, as indicated in Fig. 6.

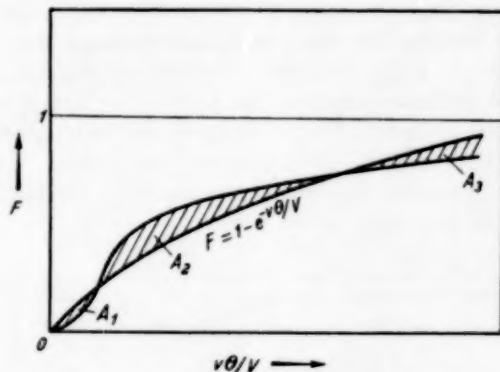


Fig. 6.

In such cases  $A_1 + A_3 = A_2$ , and the segregation is equal to  $-A_2$ .  $S$  varies from  $+1/e$  for piston-flow to values approaching  $-1$  when most of the space in the system is dead water.

The sense in which the word "mixing" has been used here should be clearly understood. We are not concerned with homogeneity, but with the age-distribution of material in the vessel and in the outgoing stream. If these distributions are the same, the system is said to be perfectly mixed, although there might, in the experiment described, be a perceptible non-uniformity of colour. On the other hand, when a fluid flows through a pipe with a high degree of turbulence, the segregation as defined above may approach that for piston-flow, although mixing in directions at right-angles to the axis of flow may be very efficient, ensuring that at any given moment the composition will be uniform across each cross-section and in the outflowing fluid.

As pointed out by GILLILAND and MASON [9], although the  $F$ -diagram for a fluidised bed may be quite close to that for perfect mixing, other tests show that longitudinal mixing is in fact not very efficient, and moreover a considerable proportion of the gas passes through the bed in the form of bubbles.

Under some circumstances, when the fluid concerned is a gas, molecular diffusion between neighbouring

elements of fluid may play a material part in determining the shape of the  $F$ -diagram. In liquids, however, diffusion coefficients are so small that only hydrodynamic effects will usually be of significance.

#### FLOW THROUGH BEDS OF SOLIDS

A very large number of chemical engineering operations involve the flow of a fluid through beds of stationary solid particles. Calculations are usually based on the assumption that piston-type flow occurs in such systems. This is certainly not exactly true, since longitudinal mixing must take place. Many cases, however, are probably amenable to the mathematical treatment which follows.

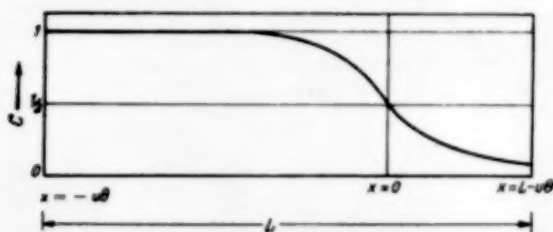


Fig. 7.

Consider a packed tubular vessel of length  $L$ , through which fluid flows with a mean axial velocity  $u$ . At time  $\theta = 0$  the colour of the fluid changes from white to red. Now if the flow were of piston-type, the plane boundary between red and white would move down the tube with velocity  $u$ . We shall denote this imaginary plane by  $x = 0$  and use it as the origin of a frame of reference moving down the tube with uniform velocity  $u$ , so that at time  $\theta$  the plane  $x = 0$  is distant  $u\theta$  from the entry, and the  $x$ -coordinates of the ends of the tube are  $(-u\theta)$  and  $(L - u\theta)$  respectively. (See Fig. 7).

The longitudinal velocity of any element of fluid relative to the plane  $x = 0$  will fluctuate irregularly. At times the element will be close to a solid surface, and viscous forces will slow it down, while at other times it will be near the centre of a channel and moving at a velocity greater than the mean; part of the time may be spent in regions of turbulence where the element will undergo rapid and irregular fluctuations in velocity. If the packing is quite randomly arranged, without any channelling, each

element of fluid will travel at the same average velocity, and will experience fluctuations of the same average magnitude and frequency. It is clear that the ordinary "random walk" theory [10] can be applied to such behaviour; the result will be redistribution of red and white material according to the laws of diffusion. That is, if  $c$  is the mean concentration (volume fraction) of red material at a plane  $x$  at time  $\theta$ ,

$$\frac{\partial c}{\partial \theta} = D \frac{\partial^2 c}{\partial x^2} \quad (15)$$

$D$  is a "diffusivity" which must be determined empirically; it will presumably depend on the viscosity, density and velocity of the liquid, and on the size and shape of the packing. The following boundary conditions will represent the facts with sufficient precision under many circumstances:

$$\left. \begin{aligned} c &= 0, x > 0, \theta = 0 \\ c &= 1, x < 0, \theta = 0 \\ c &= 0, x = \infty, \theta > 0 \\ c &= 1, x = -\infty, \theta > 0 \end{aligned} \right\} \quad (16)$$

(The above conditions hold if the concentration of white material at the entry falls virtually to zero at a time very much less than  $L/u$ . It can be shown that this will occur if  $4D/Lu < 1$ —that is, provided mixing is not too effective or the tube too short). Under these conditions the solution to (15) is

$$c = \frac{1}{2} \left[ 1 - \operatorname{erf} \left( \frac{x}{2\sqrt{D\theta}} \right) \right] \quad (17)$$

(where  $\operatorname{erf} \left( \frac{x}{2\sqrt{D\theta}} \right) = \frac{2}{\sqrt{\pi}} \int_0^{x/2\sqrt{D\theta}} e^{-y^2} dy$ ; numerical values may be found in tables and are shown in Fig. 8). Hence

$$2F(\theta) = 1 - \operatorname{erf} \left( \frac{L - u\theta}{2\sqrt{D\theta}} \right), \quad (18)$$

and since  $v/V = u/L$  ( $V$  being the void volume of the vessel):

$$2F(\theta) = 1 - \operatorname{erf} \left( \frac{1 - v\theta/V}{2\sqrt{\frac{v\theta}{V} \cdot \frac{D}{Lu}}} \right) \quad (19)$$

The  $F$ -diagram will thus be determined entirely by

the value of  $D/Lu$ . It will have the general shape shown in Figs. 1 (b) and 9.

If we let

$$\operatorname{erf}(z) = 1 - 2F \quad (20)$$

equation (19) becomes, on rearrangement,

$$\frac{1 - v\theta/V}{z\sqrt{v\theta/V}} = 2\sqrt{\frac{D}{Lu}} \quad (21)$$

(Values of  $z$  corresponding to given values of  $F$  can be found with the help of Fig. 8).

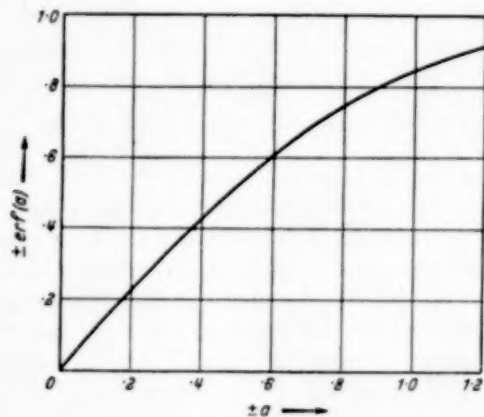


Fig. 8.  $\operatorname{Erf}(a) = \frac{2}{\sqrt{\pi}} \int_0^a e^{-y^2} dy$

For a given flow-rate and depth of packing, the left-hand side of equation (21) should be constant if the diffusion equation (15) is obeyed. However equation (21) is not very suitable for testing the diffusion hypothesis or for determining the value of  $D$  since the expression on the left-hand side is very sensitive to small errors in  $F$  over the range of greatest importance. The value of  $D$  is probably more easily determined from the slope of the  $F$ -diagram at  $v\theta/V = 1$ . Differentiating (19) with respect to  $v\theta/V$  and putting  $v\theta/V = 1$ , we find

$$\left[ \frac{dF}{d(v\theta/V)} \right]_{v\theta/V=1} = \frac{1}{2} \sqrt{\frac{Lu}{\pi D}} \quad (22)$$

$D/Lu$  can be calculated from this expression, the  $F$ -diagram calculated from equation (19), and the results compared with the experimental curve.  $D$  should, of course, be independent of  $L$  for a given  $u$ .

The hold-back in the system is equal to  $\sqrt{DV/\pi u}$ , or  $\sqrt{DL/\pi u}$ .

Fig. 9 shows the  $F$ -diagram obtained when water flowed through a bed of  $\frac{3}{8}$ -in. Raschig rings (tube diameter 4.8 cm;  $L = 140$  cm; fractional free volume 0.62; volumetric flow-rate 4.5 cc/sec). The curve calculated from equation (19) with  $D/Lu = 0.013$  is compared with the experimental points and shown to agree well.

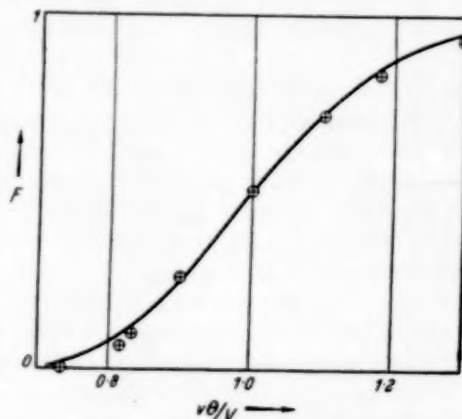


Fig. 9.  $F$ -diagram calculated for flow through packed column compared with experimental points.

The liquid running over the packing in an absorption tower is presumably subject to the same kind of mixing, although channelling may prevent equation (15) from being very closely obeyed. The quantity  $V$  in this case is equal to the total liquid hold-up.

The effect of longitudinal mixing on the performance of tubular reactors is discussed later.

#### FLOW IN PIPES

Hold-back will always arise when a true fluid flows through a pipe. In the first place, there is a variation in velocity from the axis to the wall of the pipe, so that the central "core" of fluid moves with a velocity greater than the mean, while the fluid near the wall lags behind. This effect will be most marked when flow is laminar; in turbulent flow the velocity is more uniform across the pipe, and the hold-back is less, although eddy-diffusion contributes to the longitudinal mixing. In some circumstances molecular diffusion may also contribute appreciably to the hold-back. It will be convenient to discuss laminar and turbulent flow separately.

When viscous liquids such as heavy petroleum oil or rayon dope are pumped through pipes the flow may be laminar. If the flow is changed, say, from one type of petroleum to another, or from normal to pigmented dope, the mean composition of the liquid leaving the pipe will change only gradually from one pure component to the other, and a large volume of mixed liquid will be discharged. If certain simplifying assumptions are made, the form of the  $F$ -diagram is easily calculated. (Similar calculations have been made by BOSWORTH [2], and by FOWLER and BROWN [7].)

In the first place, entrance-effects will be ignored (as in the derivation of Poiseuille's formula), and the liquid will be assumed to be everywhere in unaccelerated laminar flow with a parabolic velocity-distribution; provided the ratio of the length to the diameter of the pipe is sufficiently large ( $> 0.06 Re$ ) entrance effects will in fact be unimportant. Secondly, it will be assumed that the two liquids have the same density and viscosity, and behave as Newtonian fluids. Thirdly, molecular diffusion will be ignored.

If  $\bar{u}$  is the mean velocity and  $u$  the velocity at a distance  $r$  from the axis of a pipe of radius  $R$ , we have the well-known relationship

$$u = 2\bar{u} \left(1 - \frac{r^2}{R^2}\right). \quad (23)$$

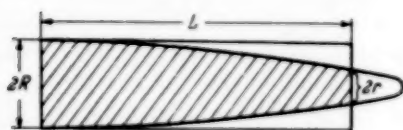
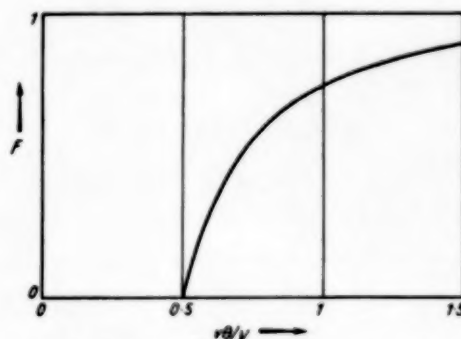


Fig. 10.

The follow-up liquid will thus first appear at the exit of a pipe of length  $L$  after a time  $L/2\bar{u}$ ; after a greater time,  $\theta$ , the situation will be as shown in Fig. 10, with a core of follow-up liquid of diameter  $2R\sqrt{1 - L/2\bar{u}\theta}$  at the exit. Allowing for the variation of velocity from the centre to the edge of the core, the fraction of follow-up liquid in the stream leaving the pipe is seen to be

$$F(\theta) = \frac{1}{\pi R^2 \bar{u}} \int_0^{R\sqrt{1 - L/2\bar{u}\theta}} 2\bar{u} \left(1 - \frac{r^2}{R^2}\right) \cdot 2\pi r \cdot dr, \quad (24)$$

$$\left. \begin{aligned} &= 1 - \frac{L^2}{4\bar{u}^2} \theta^2, \bar{u}\theta/L > \frac{1}{2} \\ &= 1 - \frac{V^2}{4V^2} \theta^2, v\theta/V > \frac{1}{2} \end{aligned} \right\}. \quad (25)$$

Fig. 11.  $F$ -diagram for viscous flow in pipe.

The resulting  $F$ -diagram is shown in Fig. 11. Its shape is independent of the length and diameter of the pipe, and of the viscosity and velocity of the fluid, (provided of course that flow is laminar). The hold-back is  $\frac{1}{2}$ . BOSWORTH [2] has calculated the effect of molecular diffusion on systems of this kind (his  $F_r$  is equivalent to the present author's  $E(\theta)$ ). He shows that it can be ignored providing the following conditions are fulfilled:

$$\left. \begin{aligned} R &> 13\sqrt{D_m L/\bar{u}} \\ L &> 6.5 \times 10^4 D_m/\bar{u} \end{aligned} \right\},$$

(where  $D_m$  is the molecular diffusivity), and points out that in the case of gases turbulence usually occurs while  $R$  is too small for the first condition to be satisfied. With liquids, however, which have much higher Schmidt numbers ( $\mu/\rho D_m$ ), there may be a considerable range of pipe-diameters for which flow is laminar and the first condition is also satisfied.

BOSWORTH [3] has also derived expressions for  $E(\theta)$  ( $F_r$  in his nomenclature) for turbulent flow in pipes, starting from simplified expressions for the values of the axial velocity and eddy-diffusivity at various distances from the pipe wall. The following expression for  $F(\theta)$  can be derived from BOSWORTH's formula:

$$\left. \begin{aligned} F(\theta) &= 1 - 2\alpha^n \times \\ &\times \left[ 1 - \beta n - \frac{1}{2}\beta - \alpha^n \left( \frac{1}{2} - \frac{5}{2}\beta n - \frac{5}{4}\beta \right) \right. \\ &\quad \left. - \beta(2n+1) \left( \alpha^{2n} - \frac{1}{4}\alpha^{3n} \right) \right] \end{aligned} \right\} \quad (26)$$



where

$$\frac{1}{x} = 2 \frac{v\theta}{V} \times$$

$$\times \left[ \left( 1 - \beta n - \beta/2 \right) \frac{n}{n-1} + \left( -\frac{1}{2} + \frac{5}{2} \beta n + \frac{5\beta}{4} \right) \times \right.$$

$$\times \left( \frac{2n}{2n-1} \right) - \beta (2n+1) \left( \frac{3n}{3n-1} + \frac{4n}{4n-1} \right) \left. \right]$$

$$\beta = (n-1)^2 R / 0.32 n L,$$

$$n = 7, 2,000 < Re < 100,000,$$

$$n = 8, Re > 100,000,$$

$R$  being the radius and  $L$  the length of the pipe.

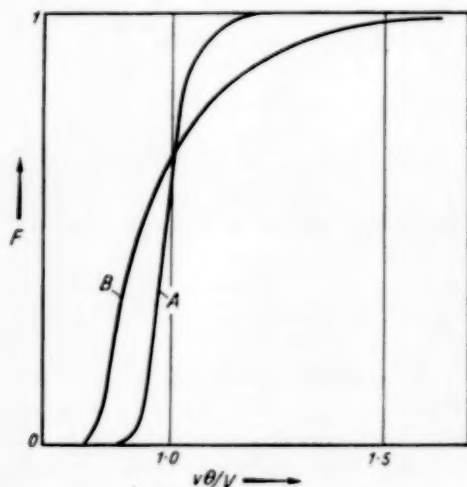


Fig. 12. Experimental (A) and calculated (B)  $F$ -diagrams. Water in circular tube,  $Re = 6940$ ,  $R/L = 6.3 \times 10^{-4}$ .

Comparison can be made with the experimental results of FOWLER and BROWN [7]. Fig. 12 shows an experimental  $F$ -diagram compared with that calculated from BOSWORTH's formula. In Fig. 13 a comparison is made between calculated and observed values of  $\frac{v}{V}(\theta_{0.8} - \theta_{0.2})$  for various Reynolds numbers in a given pipe (i.e.  $F$  has the value 0.8 at  $\theta_{0.8}$ , and the value 0.2 at  $\theta_{0.2}$ ). It will be seen that BOSWORTH's formula predicts (at least under the conditions chosen for the comparison) a much greater

degree of longitudinal mixing than is actually observed, and also that it fails to predict the marked effect of velocity of flow on the  $F$ -diagram for a given pipe.

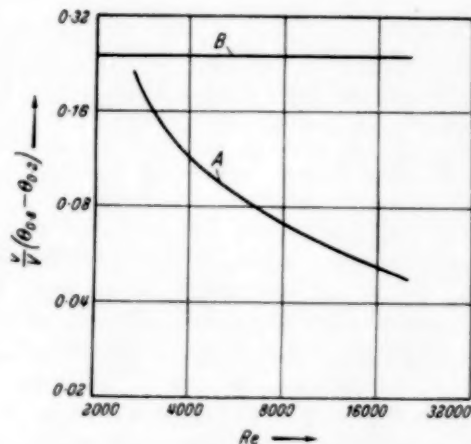


Fig. 13. Experimental (A) and calculated (B) values of  $v/V(\theta_{0.8} - \theta_{0.2})$ .  $R/L = 6.3 \times 10^{-4}$ .

## REACTORS

The performance of a steady-flow reactor can be calculated from the  $F$ -diagram provided the reaction is first-order, or pseudo-first-order, with a velocity-constant which does not vary from place to place in the reactor. For instance, if an effluent containing a radioactive element is allowed to flow through a reservoir, the concentration of the element at the exit can be calculated if its radioactive decay-constant  $k$  and the  $F$ -diagram of the system are known.

Consider those elements of fluid which have ages between  $\theta$  and  $(\theta + d\theta)$  at the exit. A fraction  $(1 - e^{-k\theta})$  of the reactant originally contained in these elements will have reacted during its passage through the vessel. Hence the total fraction  $(1 - f)$  of reactant which reacts during its passage through the vessel is

$$1 - f = \int_0^{\infty} (1 - e^{-k\theta}) E(\theta) d\theta. \quad (27)$$

From equation (3)

$$E(\theta) d\theta = dF(\theta). \quad (28)$$

Hence:

$$1 - f = \int_{\theta=0}^{\infty} (1 - e^{-k\theta}) dF(\theta) \quad (29)$$

$$= 1 - \int_{\theta=0}^{\infty} e^{-k\theta} dF(\theta).$$

$f$  can be evaluated by graphical integration if the  $F$ -diagram is available.

In the special case, previously discussed, of a tubular packed vessel, the expression for  $F$  given in equation (19) is unsuitable for use in equation (29) because of the approximations which have been made. Instead we set up the differential equation for a tubular reactor with longitudinal diffusion as well as flow (changes in volume are assumed not to occur, so that the mean longitudinal velocity,  $u$ , is the same at all cross-sections). The equation is easily shown, by making a balance on a section of differential length  $dy$ , to be

$$\frac{d^2c}{dy^2} - \frac{u}{D} \frac{dc}{dy} - \frac{kc}{D} = 0. \quad (30)$$

where  $c$  is the concentration of reactant at cross-section  $y$ . The concentration of reactant in the entering stream is  $c^*$ ; owing to diffusion the concentration just within the entrance of the reactor, at  $y = 0$ , is less than  $c^*$ . The following boundary condition expresses the fact that the rate at which reactant is fed to the reactor is equal to the rate at which it crosses plane  $y = 0$  by combined flow and diffusion.

$$uc^* = uc - D \cdot dc/dy, y = 0 \quad (31)$$

At the outlet ( $y = L$ )

$$ufc^* = uc - D \cdot dc/dy, y = L,$$

$fc^*$  being the concentration of the exit stream. Now if  $dc/dy$  were negative, the concentration in the exit stream would be greater than that at the end of the packing. If  $dc/dy$  were positive the concentration would pass through a minimum somewhere in the reactor and then rise towards the downstream end. Intuition suggests that neither of these situations can arise, so that the boundary condition must be:

$$\frac{dc}{dy} = 0, y = L. \quad (32)$$

The solution to equation (30) with these two boundary conditions is

$$\left. \begin{aligned} \frac{c}{c^*} &= \exp\left(\frac{uy}{2D}\right) \times \\ &\times \left[ \frac{2(1+a)\exp\frac{ua}{2D}(L-y) - 2(1-a)\exp\frac{ua}{2D}(y-L)}{(1+a)^2 \exp\frac{uaL}{2D} - (1-a)^2 \exp\frac{-uaL}{2D}} \right] \end{aligned} \right\} \quad (33)$$

where

$$a = \sqrt{1 + 4kD/u^2}.$$

The value of  $(1 - c/c^*)$  at the exit ( $y = L$ ) is equal to  $(1 - f)$ , the fraction reacted. Hence

$$\left. \begin{aligned} 1 - f &= 1 - \\ &\frac{4a}{(1+a)^2 \exp\frac{-uL}{2D}(1-a) - (1-a)^2 \exp\frac{-uL}{2D}(1+a)} \end{aligned} \right\} \quad (34)$$

As  $D \rightarrow 0$  this expression tends to

$$1 - f = 1 - \exp\frac{-kL}{u} \quad (35)$$

which is the well-known solution for "piston-flow." As  $D \rightarrow \infty$ , we find

$$1 - f = \frac{kL}{u + kL} \quad (36)$$

which is the solution for complete mixing. For very small values of  $D$

$$1 - f \approx 1 - (1 + k^2 DL/u^3) \exp\frac{-kL}{u}. \quad (37)$$

From this it can be seen that the effect of diffusion is to decrease the fractional conversion compared to that for piston-flow, but that the effect will be negligible provided  $k^2 DL/u^3 \ll 1$ , or  $[\ln f]^2 D/Lu \ll 1$ . Thus for specified operating conditions it is possible to decide, if an approximate value of  $D$  is available, whether neglect of longitudinal diffusion will lead to serious error in calculating the output of the reactor.

The foregoing treatment of reactors will seldom be applicable to practical problems except as a rough guide. In the first place, the heat of reaction often gives rise to temperature-gradients, and hence point-to-point variations in the value of the reaction-velocity constant, so that the chance of a molecule

reacting depends on its path through the reactor, as well as its residence-time. Secondly, if the reaction is of order other than first, the chance of a given molecule reacting depends on the molecules which it encounters in its passage through the reactor; the nature of these encounters is largely determined by diffusional processes caused by point-to-point variations in composition in the fluid, which cannot be deduced from the  $F$ -diagram. Second-order reactions between imperfectly mixed fluids have been considered by the author [5]. DENBIGH [6] has considered second-order reactions taking place in a fluid in laminar flow in a pipe, under conditions such that molecular diffusion may be ignored.

### BLENDERS

A continuous-flow blender is a mixing vessel into which flows a stream of material of continuously-varying composition. In the vessel elements of material which have entered at different times are mixed, so that the outflowing stream shows less variation in composition than the input. The case of a perfectly-mixed blender has been considered in detail elsewhere [4], with special reference to the flow of town gas through a gas-holder, and consequent smoothing-out of fluctuations in the calorific value. BEAUDRY [1] has considered the special case of a perfectly-mixed blender with a feed consisting of batches of material of finite volume. A blender which displays segregation will be less effective in reducing fluctuations than one in which perfect mixing occurs.

Suppose the concentration of some component in the entering stream has a concentration  $c_i$  which fluctuates with time. Its value at any time is  $(\bar{c} + \delta_i)$ , where  $\bar{c}$  is the mean value of  $c_i$  which is assumed to show no trend. A convenient measure of magnitude of the fluctuations in  $c_i$  is its standard deviation  $\sigma_i$ :

$$\sigma_i^2 = \overline{\delta_i^2}. \quad (38)$$

$\sigma_i$  is assumed to show no trend. The concentration  $c_0 = (\bar{c} + \delta_0)$  of the outgoing stream has a standard deviation  $\sigma_0$ . The problem is to find the ratio  $\sigma_0/\sigma_i$ . The rates of inflow and outflow are assumed constant and equal to  $v$ . The concentration  $c_0(t)$  in the outflow at time  $t$  is then given by

$$c_0(t) = \int_{\theta=0}^{\infty} c_i\{t-\theta\} E(\theta) d\theta, \quad (39)$$

where  $c_i\{t-\theta\}$  is the concentration in the inflow at time  $(t-\theta)$ . Hence

$$\delta_0(t) = \int_{\theta=0}^{\infty} \delta_i\{t-\theta\} E(\theta) d\theta \quad (40)$$

and

$$[\delta_0(t)]^2 = \left[ \int_{\theta=0}^{\infty} \delta_i\{t-\theta\} E(\theta) d\theta \right]^2. \quad (41)$$

However, it is generally true that

$$\left[ \int_0^{\infty} f(y) dy \right]^2 = 2 \int_{y=0}^{\infty} \int_{r=0}^{\infty} f(y) f(y+r) dy dr, \quad (42)$$

where  $f(y)$  is any function of  $y$ . Applying this to equation (42):

$$\left[ \delta_0(t) \right]^2 = 2 \int_{\theta=0}^{\infty} \int_{r=0}^{\infty} \delta_i\{t-\theta\} \times \delta_i\{t-\theta-r\} E(\theta) E(\theta+r) d\theta dr. \quad (43)$$

Averaging this with respect to  $t$

$$\sigma_0^2 = \overline{\delta_0^2} = 2 \int \int \overline{\delta_i\{t-\theta\} \delta_i\{t-\theta-r\}} \times E(\theta) E(\theta+r) d\theta dr. \quad (44)$$

Now the quantity

$$R(r) = \frac{\overline{\delta_i\{t'\} \delta_i\{t'-r\}}}{\sigma_i^2} \quad (45)$$

(the numerator being averaged with respect to  $t'$ ) is known as the autocorrelation coefficient or serial correlation coefficient of  $c_i$  for a time-interval  $r$ . Substituting (45) in (44) we have

$$\sigma_0^2/\sigma_i^2 = 2 \int_{\theta=0}^{\infty} \int_{r=0}^{\infty} R(r) E(\theta) E(\theta+r) d\theta dr. \quad (46)$$

$R(r)$  may be found as a function of  $r$  from a representative record of  $c_i$  vs.  $t$  in various ways which have been discussed elsewhere (4). (The relationship between  $R(r)$  and  $r$  indicates whether the fluctuations

in  $c_i$  are on the whole rapid or slow, and whether they display any regular periodicity). Assuming that  $R(r)$  is known for a sufficient range of values of  $r$ , in order to evaluate the integral in (46) it is necessary to know  $E(\theta)$  as a function of  $\theta$ . The necessary information is contained in the  $F$ -diagram of the system, and the following is perhaps the simplest way of doing the calculation. First fit some simple function of  $\theta$  (such as a power-series) to the  $F$ -diagram up to a value  $\theta_1$ , at which  $F(\theta_1)$  is very close to 1. Differentiate this function with respect to  $\theta$ . From equation (3) we see that

$$\frac{dF(\theta)}{d\theta} = E(\theta), \quad (47)$$

so that  $E(\theta)$  is now a known function of  $\theta$ . For a given value of  $\theta$ ,  $E(\theta + r)$  is the value obtained by replacing  $\theta$  by  $(\theta + r)$ . It will now be possible to evaluate the integral

$$I(r) = \int_{\theta=0}^{\theta_1} E(\theta) E(\theta + r) d\theta \approx \int_{\theta=0}^{\infty} E(\theta) E(\theta + r) d\theta \quad (48)$$

algebraically for a number of values of  $r$ . The integral

$$\sigma_0^2/\sigma_i^2 = 2 \int_{r=0}^{\infty} R(r) I(r) dr \quad (49)$$

can now be evaluated graphically. (In practice, of course, the upper limit will be taken at some value of  $r$  for which the integrand has become vanishingly small).

#### THE USE OF MODELS FOR PREDICTING $F$ -DIAGRAMS

Under certain circumstances the  $F$ -diagram of a large system can be predicted with confidence from that for a model. The conditions to be fulfilled are (a) The model must be geometrically similar to the system; (b) The Reynolds number must be the same in the model and the system; (c) Gravity-waves, density-differences, surface tension, and other influences apart from inertia and viscosity, must be unimportant in determining the behaviour of the fluid in both model and system.

In the simple case of a fluid flowing through a tank or a fixed bed of solids, the same fluid being used in

the model as in the system, equality of the Reynolds numbers requires that

$$\frac{v_1}{v_2} = \frac{L_1}{L_2} \quad (50)$$

where  $v_1, v_2$  are the volumetric flow-rates and  $L_1, L_2$  the linear dimensions of the model and system respectively. That is, in a 1/10 scale model the volumetric flow-rate must be 1/10 that in the full-scale system. If the system incorporates a rotating stirrer, the angular velocities,  $\omega$ , of the stirrers in model and system are related by

$$\frac{\omega_1}{\omega_2} = \left(\frac{L_2}{L_1}\right)^2 \quad (51)$$

In the 1/10 scale model the stirrer must rotate 100 times as fast as in the system.

If these conditions are fulfilled the flow-patterns of the fluid will be geometrically similar in model and system, hence both will have the same  $F$ -diagram.

The simple type of model experiment described here cannot be applied to systems in which the fluid is of non-uniform density or viscosity owing to variations in temperature or composition from point to point, or to fluidised beds.

#### REFERENCES

- [1] BEAUDRY, J. P.; Chem. Eng. 1948 55 112. [2] BOSWORTH, R. C. L.; Phil. Mag. 1948 39 847. [3] BOSWORTH, R. C. L.; Phil. Mag. 1949 40 314. [4] DANCKWERTS, P. V. and SELLERS, E. S.; Ind. Chemist 1951 27 395; Coke and Gas 1952 14 247. [5] DANCKWERTS, P. V.; Appl. Sci. Res. A 1952 3 279. [6] DENBIGH, K. G.; J. Appl. Chem. 1951 1 227. [7] FOWLER, F. C. and BROWN, G. G.; Trans. Amer. Inst. Chem. Eng. 1943 39 491. [8] GILLILAND, E. R. and MASON, E. A.; Ind. Eng. Chem. 1949 41 1191. [9] GILLILAND, E. R. and MASON, E. A.; Ind. Eng. Chem. 1952 44 218. [10] KENNARD, E. H.; Kinetic Theory of Gases, 1938 New York, McGraw-Hill, p. 268. [11] HULL, D. E. and KENT, J. W.; Ind. Eng. Chem. 1952 44 2745. [12] HULL, D. E., KENT, J. W. and LEE, R. D.; World Oil 1949 129 188. [13] SMITH, S. S. and SCHULZE, R. K.; Petroleum Eng. 1948 19 94; 1948 20 330. [14] LAPIDUS, L. and AMUNDSON, N. R.; J. Phys. Chem. 1952 56 984. [15] BERNARD, R. A. and WILHELM, R. H.; Chem. Eng. Prog. 1950 46 233. [16] ARTHUR, J. R., LINETT, J. W., RAYNOR, E. J. and SINGTON, E. P. C.; Trans Faraday Soc. 1950 46 270. [17] MORALES, M., SPINN, C. W. and SMITH, J. M.; Ind. Eng. Chem. 1951 43 225.

#### NOTE ADDED IN PROOF

*Flow in Pipelines*—HULL and KENT [11] have recently published an account of experiments on petroleum flowing in



a 182-mile long 10-inch diameter pipe line. A radioactive tracer was used to obtain (in effect) C-diagrams for various lengths of pipe. With a Reynolds Number of 20,000-30,000 the diagrams obtained were close to those which would be expected if the "diffusion" equation (15) were followed,  $D$  having a value of 1.3 sq. ft./sec. Further experimental work on mixing in pipe-lines is referred to by the authors [12], [13].

**Flow in Packed Beds**—LAPIDUS and AMUNDSON [14], have analysed the consequences of longitudinal mixing in adsorption columns. BERNHARD and WILHELM [15] have measured the apparent radial diffusivity in fluids flowing through beds of solids. It seems likely that the longitudinal diffusivity  $D$  (equation (15)) will have a different value. ARTHUR *et al.* [16] and MORALES *et al.* [17] have shown that the fluid velocity differs markedly from the mean in the neighbourhood of the wall of the column.

# NOTATION.

$A$  = area under curve

$c$  = concentration

$C(\theta)$  = concentration at exit of vessel at time  $\theta$ .

$c^*$  = concentration of stream entering reactor

$D$  = apparent diffusivity

$D_m$  = molecular diffusivity

$E(\theta)$  = distribution-function for residence-times  $\theta$

$$\operatorname{erf}(z) = \frac{2}{\sqrt{\pi}} \int_0^z e^{-y^2} dy$$

$F(\theta)$  = fraction of material in outflow which has been in system for a time less than  $\theta$

$f$  = fraction of reactant unreacted

$H$  = hold-back (equation (14))

$I(\theta)$  = distribution-function for "ages,"  $\theta$ , of material in system

$k$  = first-order reaction-velocity constant

$L$  = length of tube or reactor

$n$  = parameter in equation (26)

$Q$  = quantity of tracer material injected

$R$  = radius of pipe

$R(r)$  = serial correlation-coefficient of  $c_i$  for time-interval  $r$

$r$  = radial distance from tube-axis; or time-interval

$Re$  = Reynolds number

$S$  = segregation (Figs. 4, 5, 6)

$t$  = time

$u$  = velocity of flow

$\bar{u}$  = mean velocity of flow in open pipe

$V$  = volume of vessel

$v$  = volumetric flow-rate

$x$  = distance referred to coordinates moving with velocity  $u$

$y$  = distance referred to stationary coordinates

$z$  = defined by equation (20)

$\alpha$  = parameter in equation (26)

$\beta$  = parameter in equation (26)

$\delta_i, \delta_0$  = instantaneous deviations of  $c_i, c_0$  from  $\bar{c}$

$\theta$  = time-interval, residence-time or "age"

$\sigma_i, \sigma_0$  = standard deviations of  $c_i, c_0$  from  $\bar{c}$

$\omega$  = angular velocity

## Extraction of acetic acid from water. 1—benzene-acetic acid-water

F. H. GARNER, S. R. M. ELLIS and U. N. G. ROY

The Chemical Engineering Dept., The University, Birmingham, 15

(Received 4 November, 1952)

**Summary**—Liquid-liquid equilibrium data are given for the system benzene-acetic acid-water at 30°C, 40°C, 50°C and 60°C. The experimental distribution coefficients are in close agreement with those predicted from binary vapour-liquid equilibrium data; Other papers are to follow giving liquid-liquid and vapour-liquid equilibrium data for the system ethyl acetate-acetic acid-water.

**Résumé**—Présentation de données expérimentales sur l'équilibre liquide-liquide dans le système benzène-acide acétique—eau à 30°C, 40°C, 50°C et 60°C. Les coefficients de partage expérimentaux sont en accord étroit avec les valeurs calculées à partir des données d'équilibre liquide-vapeur des systèmes binaires. Les résultats d'équilibre liquide-liquide et liquide-vapeur pour le système acétate d'éthyle-acide acétique-eau, seront publiés ultérieurement.

### Introduction

The strong affinity of acetic acid for water from which it cannot be easily separated has led to a considerable amount of research into the problem of devising separation methods that can be economically used by industry. Large quantities of acetic acid in aqueous solution are produced in the form of pyroligneous acid from the wood distillation industry, and, in still weaker form, from fermentation processes. Large quantities of glacial acetic acid used in the cellulose acetate industry undergo dilution and require concentration before they can be reused.

GOERING [1] in 1883 applied liquid-liquid extraction to the concentration of acetic acid from aqueous solutions. The solvent used was ethyl acetate and GOERING drew attention to the fact that change in temperature had little effect on the extraction process. RICARD and GUINOT [2] and DREYFUS and HANEY make use of a second liquid solvent such as a hydrocarbon to reduce the solubility for water of the solvent layer. OTHMER, WHITE and TRUEGER [3] provide a large amount of information on the use of different solvents for extracting acetic acid from water.

B.I.O.S. Report 1051 mentions the use of a solvent 85% ethyl acetate, 15% benzene. An interesting observation is the power of traces of methylene chloride in aiding the separation of ethyl acetate from water [4].

Ternary liquid-liquid equilibrium data has been published for systems involving acetic acid, water, and a large number of solvents including chloroform, isopropyl ether, methyl isobutyl ketone, benzene, ethyl

acetate, etc. TREYBAL [9] has shown a large discrepancy between the predicted and experimental results for the system benzene-acetic acid-water.

The purpose of this first paper is to present new experimental data for the system benzene-acetic acid-water at a range of temperatures and to compare the experimental and predicted distribution coefficients.

### Determination of Solubility Curve

The apparatus used to determine the solubility curve was essentially a thin walled glass tube, fitted with a cork through which is introduced a glass stirrer and thermometer graduated in tenths of a degree centigrade. Through another hole in the cork a burette is introduced so that the tip of the burette is just projecting beyond the cork. The apparatus was placed in a thermostat controlled to  $\pm 0.1^\circ\text{C}$  with illuminated windows to view the experiment. Weighed miscible mixtures were placed in the test tube and titrated to turbidity with a third component.

### Determination of Tie Lines

For acetic acid-benzene-water at 30°C and 40°C the apparatus described by HUNTER and NASH [5] was inserted in a large thermostatic bath and used for the determination of tie lines. At temperatures of 50°C and 60°C the liquid mixture was weighed in a stoppered flask and introduced into the constant temperature bath. The flask was agitated thoroughly every 15 minutes for 3-4 hours. After standing over night samples were then drawn off from the two layers.

VOL.  
2  
1953

### Purity of Reagents

**Water**—Distilled water was treated with solid barium hydroxide to remove any carbon dioxide.

**Acetic acid**—Analar acetic acid was fractionated with ethylene dichloride and then stored in the absence of moisture. B.P. 118-15°C.

**Benzene**—The purification of benzene was effected in a thirty plate column at a reflux ratio of 25 : 1. The boiling point at 760 mm was 80.1°C and the refractive index  $D_{20}^{20}$  1.5011.

### Analysis of Acetic Acid

A volumetric method of analysis was used where a dilute solution of acetic acid was titrated with standard carbonate free barium hydroxide. Phenolphthalein was used as the indicator.

### Results

Solubility curve and tie line data are given on Tables 1 and 2. Fig. 1 shows the solubility and tie line data at 30°C represented on a triangular graph.

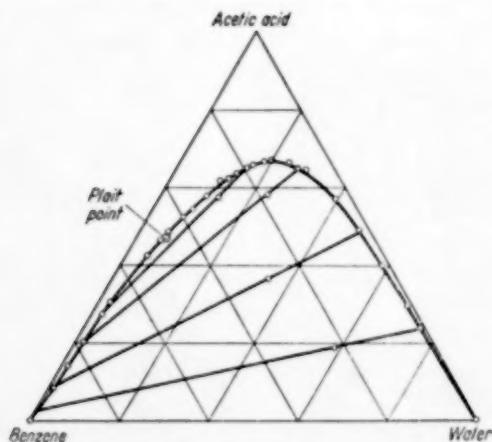


Fig. 1

### Discussion of Results

A comparison of the results of Tables 1 and 2 shows that the spread of the solubility curve decreases only slightly with temperature. The distribution coefficient shows only a small variation with temperature when the concentration of acetic acid in the water layer is less than 50.0% by weight. Above this concentration of acetic acid in water the distribution coefficient varies more widely with temperature.

The tie line data is satisfactorily correlated by BACHMAN [6] and OTHMER-TOBIAS [7] plots.

On Fig. 2 a plot has been made of the mol fraction of acetic acid in the benzene layer against the mol fraction of acetic acid in the water layer. The resulting distribution coefficients are slightly lower than those reported by HAND [8]. TREYBAL [9] states that predicted distribution coefficients from the available vapour-liquid equilibrium data were considerably

Table 1. Acetic Acid-Water-Benzene—Solubility Data

t°C	Acetic acid gm	Water gm	Benzene gm	t°C	Acetic acid gm	Water gm	Benzene gm
30.0	29.8	69.4	0.4	50.0	40.7	57.3	2.0
	39.6	59.2	1.2		49.8	47.5	2.7
	48.7	49.1	2.2		57.7	36.2	6.1
	57.2	39.2	3.6		64.0	25.2	10.8
	64.2	29.0	6.8		59.2	13.9	26.9
	66.7	18.3	15.0		47.7	8.0	44.3
	62.0	12.6	35.4		35.6	3.6	60.8
	48.2	6.3	45.5		41.0	4.8	54.2
	42.6	4.7	52.7		48.9	7.9	43.2
	46.7	5.8	47.5		55.5	11.3	33.2
	52.0	8.0	40.0		60.9	15.0	24.1
	54.3	9.0	36.7		63.5	21.1	15.4
	57.8	10.4	31.8		63.0	25.9	11.1
	61.5	11.3	27.2		60.1	32.6	7.3
	63.7	13.9	22.4		25.3	3.3	71.4
	65.7	16.3	18.0		26.0	71.7	2.3
	66.0	24.5	9.5				
	62.7	31.7	5.6				
	50.2	48.0	1.8				
	14.0	1.1	84.9				
	30.2	2.5	67.3				
40.0	42.5	4.9	52.6	60.0	40.6	5.6	53.8
	50.6	8.0	41.4		48.2	9.1	42.7
	57.4	11.0	31.6		54.4	13.2	32.4
	62.8	14.8	22.4		59.9	16.3	23.8
	64.8	21.4	13.8		62.2	23.1	14.7
	64.2	26.6	9.3		60.6	28.8	10.6
	59.8	34.8	6.4		54.6	39.2	6.2
	40.8	57.5	1.7		40.1	56.5	3.4
	50.0	47.5	2.5		49.5	46.0	4.5
	58.5	36.6	4.9		57.1	35.6	7.3
	64.7	26.0	9.3		61.9	25.1	13.0
	61.5	14.5	24.0		55.8	13.3	39.9
	39.4	3.8	56.8		44.0	7.5	48.5
	51.9	8.8	39.3		30.4	3.6	66.0
	28.5	2.5	69.0		22.8	3.3	73.9
	28.1	70.3	1.6		23.1	74.1	2.8
	15.2	1.7	73.1				

higher than the experimental values of HAND [8]. It was thought these discrepancies might be due to

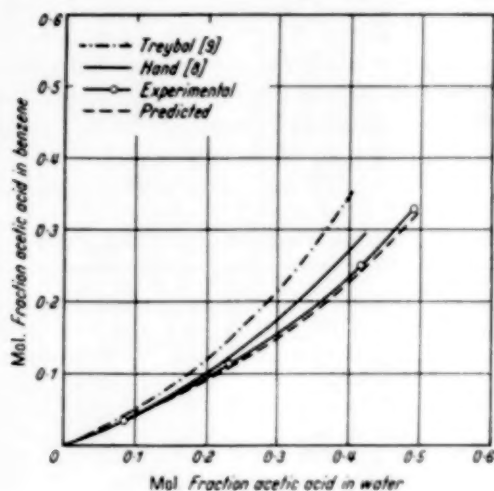


Fig. 2

inaccurate vapour-liquid equilibrium data for the benzene-acetic acid system and thus in this paper new equilibrium data has been used to predict the distribution coefficients.

#### Prediction from Binary Vapour-Liquid Equilibria

At equilibrium the activities of acetic acid in the two phases are equal

$$x_1 \gamma_1 = x_2 \gamma_2$$

where  $x_1$  = mole fraction of acetic acid in benzene.

$x_2$  = mole fraction of acetic acid in water.

$\gamma_1 \gamma_2$  = activity coefficients of acetic acid in benzene and water respectively.

If the partition or distribution coefficient is defined as  $K$  then

$$K = \frac{x_1}{x_2} = \frac{\gamma_2}{\gamma_1}$$

Table 2. Acetic Acid-Water-Benzene Tie Line Data

t°C	Overall composition			% acid in water rich phase	% acid in benzene rich phase	Plait point		
	% acid	% benzene	% water			% acid	% benzene	% water
30.0	18.6	22.8	58.6	23.4	2.3	46.8	46.8	6.4
	36.2	29.0	34.8	48.8	8.7			
	57.8	17.7	24.5	64.6	20.1			
	57.0	30.0	13.0	73.5	28.0			
40.0	11.3	57.0	31.7	23.5	2.4	47.1	45.5	7.4
	26.6	41.7	31.7	42.5	6.7			
	35.0	30.5	34.5	47.5	8.3			
	40.0	34.5	25.5	56.0	12.4			
	48.7	41.0	10.3	64.0	22.0			
	53.0	28.6	18.4	64.1	22.5			
50.0	6.25	46.2	47.5	11.1	0.62	47.8	44.2	8.0
	16.4	39.9	43.7	25.6	2.9			
	36.5	29.4	34.1	48.5	9.3			
	46.8	24.7	28.5	57.2	14.6			
	57.5	22.1	20.4	63.5	23.7			
60.0	5.8	43.4	50.8	8.8	0.56	48.2	42.9	8.7
	15.4	34.8	49.8	22.4	2.34			
	25.8	35.8	38.9	36.5	5.7			
	34.2	32.8	33.0	47.0	8.75			
	51.0	28.9	20.1	61.3	22.0			

In the above table all percentages are by weight



Table 3

Mole % in Benzene Phase			Mole % in water phase			Experimental distribution coefficient	Predicted distribution coefficient
Acetic acid	Benzene	Water	Acetic acid	Benzene	Water		
31.2	61.3	7.5	45.0	8.5	46.5	0.68	0.66
23.5	69.6	6.9	40.0	4.0	56.0	0.60	0.56
10.5	85.4	4.1	22.8	76.5	0.7	0.48	0.45
3.1	95.2	1.7	9.0	0.2	90.8	0.38	0.38

The activity coefficient of the solute in ternary mixtures can be predicted from binary vapour-liquid equilibrium data by linear interpolation or by the use of Margules, Van Laar, or other ternary equations. The fact that the vapour-liquid equilibrium data is determined at a different temperature to the liquid-liquid equilibrium does not in general greatly influence the predicted distribution coefficient, since the ratio of the activity coefficient varies only slightly with temperature.

A difficulty in this particular application of predicting the activity coefficient of acetic acid in the benzene rich layer is the possibility of association of the acetic acid to give the dimer. HAND [8], however, has shown that the simple distribution law for acetic acid in benzene holds in concentrated solutions but breaks down in dilute solutions. He has therefore postulated the presence of water in the benzene layer breaks down the association of acetic acid to give the monomer. Accordingly the vapour-liquid equilibrium and liquid-liquid equilibrium data have been based on a MW of 60 for acetic acid.

In these laboratories PEARCE [10] has recently investigated the vapour-liquid equilibrium data of the system benzene-acetic acid. This data is in agreement with that of ROSANOFF and EASLEY [11] when based on the same molecular weight for acetic acid. They used a molecular weight of approximately 100 for acetic acid, this being calculated from the vapour densities of acetic acid.

We have used the vapour-liquid equilibrium data of OTHMER and GILMOT [12] for the system acetic acid-water.

Thus using the method of linear interpolation as proposed by CARLSON and COLBURN [13] it can be

seen from Fig. 2 that the new experimental results are in close agreement with the predicted values. This agreement is perhaps best illustrated by Table 3.

From Fig. 2 it can also be seen that there is a large difference between the predicted results of TREYBAL [9] and those given in this paper. It would appear that TREYBAL has used vapour-liquid equilibrium data for the system acetic acid-benzene based on a molecular weight of approximately 100, and for the system acetic acid water based on a molecular weight of 60.0. As close agreement as shown on Table 3 can be obtained by using a molecular weight of 100 for both binary systems.

The general conclusion of this work is that the experimental distribution coefficient for acetic acid in benzene and water is slightly lower than that reported by HAND [8] but is in close agreement with predicted distribution coefficients calculated from vapour-liquid equilibrium activity coefficients. Further, the distribution coefficients are relatively constant for temperature changes of 30°C to 60°C.

#### REFERENCES

- [1] GOERING, T.; GP. 28064. [2] RICARD, M., GUINOT, H. M.; U.S.P. 2,317,758. [3] OTHMER, D. F., WHITE, R. E., TRUEGER, E.; Ind. Eng. Chem. 1941 **33** 1240. [4] Fiat Report 144. [5] HUNTER, T. G., NASH, A. W.; Ind. Eng. Chem. 1935 **27** 836. [6] BACHMAN, I.; Ind. Eng. Chem. Anal. Ed. 1940 **12** 38. [7] OTHMER, D. F. and TOBIAS, P. E.; Ind. Chem. Eng. 1942 **34** 696. [8] HAND, D. B.; J. Phys. Chem. 1930 **34** 1961. [9] TREYBAL, R. E.; Ind. Eng. Chem. 1944 **36** 875. [10] PEARCE, C. J.; M.Sc. Thesis 1952 Birmingham University. [11] ROSANOFF, M. A. and EASLEY, C. W.; J. Amer. Chem. Soc. 1909 **31** 986. [12] OTHMER, D. F. and GILMOT, R.; Ind. Eng. Chem. 1944 **36** 1061. [13] CARLSON, H. C. and COLBURN, A. P.; Ind. Eng. Chem. 1942 **34** 581.

## The absorption of chlorine from air by solution of 2-ethyl hexene-1 in carbon tetrachloride

G. H. ROPER

School of Chemical Engineering, N.S.W. University of Technology, Broadway, N.S.W.

(Received 19 August 1952)

**Summary**—The disc column designed by STEPHENS and MORRIS [14] is used to study the rates of absorption of chlorine from air into solutions of 2-ethyl-hexene-1 in carbon tetrachloride. The olefin bulk concentration  $C_B$  is varied from zero to 0.034 lb. mol per ft.<sup>3</sup>, the reaction rate constant  $k_c$  in the ratio 20 : 1 by varying the concentration of the catalyst (iodine) from zero to 0.001 lb. mol per ft.<sup>3</sup>, the ratio of the bulk concentration of the olefin  $C_B$  to the concentration of dissolved chlorine at the interface  $C_i$  from zero to 280.

The fractional increase in the liquid film coefficient due to chemical reaction varies from zero to 19, and was found to be :

$$\frac{k_L}{k'_L} - 1 = 39.2 \left[ \frac{(C_C + 0.00005) C_B}{C_i} \right]^{0.5} \quad (A)$$

where  $k_L$  is the liquid film coefficient and  $k'_L$  is the coefficient for physical absorption at the same liquor rate, and  $C_C$  is the concentration of iodine, lb. mol per ft.<sup>3</sup>.

Additional data are presented for the gas film coefficients of the disc column, based on the rates of evaporation of water and of carbon tetrachloride.

**Résumé**—A l'aide de la colonne à disques de STEPHENS et MORRIS [14] l'auteur étudie la vitesse d'absorption du chlore mélangé à l'air par des solutions d'éthyl 2 hexène 1 dans  $\text{CCl}_4$ . La concentration globale  $C_B$  d'oléfine varie entre 0 et 0,034 lb. mol/ft.<sup>3</sup> (0,54 mol gr/lit.) ; la constante de réaction  $k_c$  est variée dans le rapport de 20 à 1 en modifiant la concentration du catalyseur (iode) entre 0 et 0,001 lb. mol/ft.<sup>3</sup> (0,016 mol gr/lit.) Le rapport entre les concentrations  $C_B$  et celle du chlore dissous à la couche de passage varie entre 0 et 280.

Le coefficient d'échange liquide  $K_L$  du à la réaction chimique variant entre 0 et 19, on trouve la relation (A), où  $k_L$  est le coefficient d'échange du à l'absorption physique et  $C_C$  la concentration en iode.

A partir des vitesses d'évaporation pour l'eau et  $\text{CCl}_4$ , l'auteur présente des données sur le coefficient d'échange gazeux pour le colonne à disque.

### INTRODUCTION

For physical absorption design procedures are based on the two-film theory of BRUNNER [1] and WHITMAN [15] for mass transfer. There are no general equations available relating the properties of the equipment, of the materials used and the gas and liquor rates, so that each system has its own equations characterising its performance. When the complication of a reaction in the liquid phase is encountered there is no design method available because theoretical treatment has been made for special cases only, and for these cases the theory has not been tested. The most reliable method for good design of chemical absorption equipment is to determine the overall mass transfer data from the operation of semi-works scale towers, as has been done by RIGGLE and TEPE [10] for the absorption

of chlorine in ferrous sulphate solutions and by SPECTOR and DODGE [13] for the preparation of carbon dioxide-free air using hydroxide solutions.

Theoretical studies have been made of the case of a gaseous solute of limited solubility diffusing into a liquid solution, one component  $B$  of which reacts with the gaseous solute  $A$ , [4], [12]. The reaction may be first or second order, but must be irreversible. The rate of diffusion of the gaseous solute  $A$  into an element of the liquid film at a distance  $x$  from the gas-liquid interface is :

$$N_A = -A D_A \frac{d C_A}{d x} \quad (1)$$

The rate of elimination of the gaseous solute in any element of thickness  $dx$  is  $k_c C_B C_A A dx$ . The rate of

VOL.  
2  
1953

diffusion out of the element of the liquid film is:

$$N_A = -A D_A \left( \frac{dC_A}{dx} + \frac{d^2 C_A}{dx^2} dx \right) \\ = -A D_A \frac{dC_A}{dx} - k_c C_B C_A A dx \quad (2)$$

The solutions of equations (1) and (2) have been accomplished for the case in which the reaction is instantaneous. The liquid film coefficient for chemical absorption  $k_L$  is:

$$k_L = k'_L \left[ 1 + \frac{D_B}{D_A} \cdot \frac{C_B}{C_i} \right] \quad (3)$$

where  $k'_L$  is the liquid film coefficient for physical absorption under the same operating conditions. For other rates of reaction, the chemical absorption coefficient may be expressed as an indefinite function of a number of variables, viz:

$$k_L = f(Re_L, Sc_L, k_c, C_B, C_i, D_B, D_A) \quad (4)$$

Previous experimental determinations confirm the dependence of the rate of chemical absorption on some of the factors listed in equation (4). The effect of the Reynolds number  $Re_L$  has been examined by a number of workers [2], [3], [10], [13], [14].

JENNY [8], using a stirred batch absorber, found that the rate of absorption of ethyl acetate in water was unaffected by the presence of sodium hydroxide, and that appreciable time was needed for the reaction between the ester and the alkali to go to completion. The reaction between methyl formate and sodium hydroxide in aqueous solution is fast. An increase in the caustic strength of the liquor in the absorber increases the absorption rate. The results lend qualitative support to the theory that an increase in the reaction rate constant will increase the liquid film coefficient.

A number of papers report data showing that the concentration of the liquid phase reactant has a large effect upon the rate of absorption. The absorption of chlorine in ferrous chloride solutions was studied by STEPHENS and MORRIS [14] using a disc column. The effect of the ferrous chloride concentration  $C_B$  cannot be separated from the effect of the concentration of dissolved chlorine at the interface,  $C_i$ . They varied the ratio  $C_B/C_i$  from zero to 1,200. The fractional increase in the liquid film coefficient due to the reaction was found to be:

$$\frac{k_L}{k'_L} - 1 = 0.75 \left( \frac{C_B}{C_i} \right)^{0.83} \quad (5)$$

The rate of absorption of carbon dioxide in alkaline hydroxide solutions increases with hydroxide concentrations at low concentrations [6], [8], [13], [16]. The rate of absorption of carbon dioxide in other alkaline solutions is inconclusive, but it appears that an increase in pH is accompanied by an increase in absorption rate [2], [3], [5], [6], [16].

There are no reported data showing the effect of variations in the diffusivity of the reactants or of variations in the Schmidt number upon the rate of chemical absorption.

#### *The system chlorine, 2-ethyl hexene-1, and carbon tetrachloride*

The absorption of chlorine in solutions of 2-ethyl hexene-1 and carbon tetrachloride offers certain advantages. The materials used are definite compounds with known properties. By keeping the concentrations of the solutes low the physical properties of the solutions are similar to those of the solvent. The concentrations are easily controlled and estimated. The specific reaction rate may be altered by the presence of a homogeneous catalyst (iodine) forming an interhalogen compound. The increase in the specific reaction rate is expected to be proportional to the concentration of the iodine intermediate compound, which, in turn, is expected to be proportional to the iodine concentration.

#### EXPERIMENTAL PROCEDURE AND RESULTS

**Apparatus**—A laboratory column with characteristics comparable to commercial packed towers was recently reported by STEPHENS and MORRIS [14]. The form of the column used consists of 31 carbon discs, 1.45 to 1.5 cm diameter and 0.44 to 0.46 cm thickness. The discs are threaded edgewise on 2 mm diameter glass rod and maintained at right angles by means of a styrene-butadiene co-polymer cement. The general arrangement is shown in Fig. 1.

#### GAS FILM COEFFICIENTS. THE EVAPORATION OF WATER AND OF CARBON TETRACHLORIDE

In order to evaluate the liquid film coefficients for the absorption of chlorine, it is necessary to correct the overall coefficients  $K_G$  by the relationship

$$1/H k_L = 1/K_G - 1/k_G \quad (6)$$

The gas film coefficients for the absorption of chlorine from air were estimated on the basis of a general equation derived from measured rates of evaporation of water and carbon tetrachloride.

Table 1. Vaporisation of water

Run No.	Water rate lb./hr.(ft).	Air velocity ft./sec.	Water temp. °F.		Air temp. °F.		Air R.H. %		Vaporisation rate 10 <sup>-3</sup> lb./hr.	Driving force 10 <sup>2</sup> ΔP <sub>Lm</sub> .	k <sub>G</sub>
			in	out	in	out	out	in			
1	7.9	0.370	71.1	69.6	72.8	71.3	91	60	2.15	0.43	0.151
2	16.6	0.370	68.2	68.1	69.7	69.1	96	60	2.59	0.35	0.224
3	25.0	0.370	68.5	68.4	70.0	69.3	96	64	2.41	0.33	0.221
4	37.9	0.370	69.6	69.4	71.0	69.8	94	61	2.55	0.40	0.192
5	60.6	0.370	69.8	68.0	70.6	69.2	98	63	2.68	0.27	0.299
6	81.0	0.370	70.0	70.0	70.4	68.5	98	68	2.63	0.29	0.274
7	121	0.370	66.7	66.7	69.0	69.0	97	63	2.33	0.27	0.260
8	161	0.370	67.6	67.6	69.1	69.0	97	61	2.46	0.31	0.240
9	244	0.370	68.0	68.0	69.6	69.0	97	62	2.55	0.31	0.248
10	408	0.370	69.4	69.4	69.9	68.5	98	65	2.50	0.29	0.260
11	408	0.511	70.9	71.1	72.7	72.1	95	56	4.18	0.46	0.244
12	244	0.511	71.6	71.6	73.0	72.3	96	59	4.06	0.41	0.299
13	161	0.511	72.1	72.1	73.4	72.8	95	60	3.88	0.44	0.266
14	121	0.511	72.1	72.1	73.0	71.9	96	62	3.82	0.41	0.282
15	81.0	0.511	72.3	72.0	73.0	72.8	94	56	4.12	0.49	0.254
16	81.0	0.680	72.1	71.6	73.5	73.2	91	57	4.92	0.55	0.270
17	81.0	0.972	72.9	72.1	73.5	73.6	89	58	6.46	0.60	0.325
18	81.0	1.58	73.4	72.1	74.0	73.9	85	59	8.97	0.67	0.404
19	81.0	2.17	72.7	71.2	73.6	74.1	83	59	10.2	0.66	0.468
20	81.0	3.60	73.2	71.4	74.0	74.3	83	59	15.3	0.66	0.700
21	81.0	4.97	73.2	71.4	74.0	74.0	82	59	24.7	0.69	1.08
22	121	0.511	73.6	73.2	73.6	73.6	93	58	3.82	0.53	0.218
23	121	0.972	73.8	73.4	73.9	73.2	93	59	7.39	0.53	0.421
24	121	1.58	74.3	73.4	74.1	73.2	89	60	10.4	0.64	0.491
25	121	2.17	73.6	73.0	74.3	73.8	85	61	11.6	0.68	0.514
26	121	3.00	73.9	72.7	74.3	74.0	86	64	14.5	0.61	0.714
27	121	4.97	74.3	72.5	74.6	74.1	84	64	24.7	0.67	1.11
28	408	0.680	73.6	73.6	74.6	74.3	98	64	5.15	0.34	0.456
29	408	3.00	74.1	73.8	74.3	74.7	94	60	17.5	0.44	1.20
30	408	2.17	69.8	69.8	71.3	72.5	95	67	10.6	0.31	1.03
31	408	1.58	70.7	70.7	72.1	73.4	94	66	7.89	0.36	0.661
32	408	0.972	71.1	71.1	73.0	73.6	97	65	6.16	0.30	0.621
33	244	3.09	71.4	71.4	72.9	73.5	89	68	12.1	0.47	0.771
34	244	2.17	71.6	71.6	72.9	73.6	94	67	11.3	0.37	0.927
35	244	1.58	72.1	72.1	73.3	73.6	95	68	8.48	0.35	0.734
36	244	0.972	72.4	72.4	73.4	73.2	98	68	6.23	0.28	0.671
37	244	0.680	72.8	72.8	73.9	73.6	99	69	4.54	0.35	0.391
38	161	3.00	73.4	73.4	75.5	77.6	85	47	22.9	0.75	0.921
39	161	2.17	75.0	75.0	76.4	77.9	86	57	12.7	0.69	0.555
40	161	0.972	73.1	73.1	76.3	76.7	88	66	7.64	0.51	0.451
41	161	0.680	72.6	72.6	78.2	78.0	89	58	7.31	0.54	0.409
42	161	0.511	77.2	77.2	79.7	80.4	88	45	5.56	0.84	0.200
43	81.0	3.00	70.5	70.5	74.1	90.8	77	30	15.4	0.82	0.506
44	81.0	3.81	69.5	69.5	74.5	79.6	72	46	39.4	0.77	1.54
45	81.0	10.1	71.6	71.6	73.9	74.0	80	51	23.4	0.80	0.882



Table 2. Vaporisation of carbon tetrachloride

Run No.	$\Gamma$ lb./ (hr.) (ft.)	$r$ f.p.s. (mean)	CCl <sub>4</sub> temperature °F.		Gas temperature °F.		$10^3 N_A$ lb. mol hr.	$\Delta P_{L,m}$	$k_G$
			in	out	out	in			
1	103	0.405	84.6	76.0	84	84	2.55	0.075	0.185
2	258	0.405	84.0	79.0	82	85	2.62	0.070	0.203
3	103	10.0	85.0	60.3	73	86	16.4	0.121	0.878
4	258	10.0	84.3	59.0	72	83	20.8	0.110	1.02
5	103	2.00	84.8	71.5	78	85	6.46	0.095	0.368
6	258	2.00	84.2	74.0	77	84	7.40	0.088	0.456

In all runs, air was passed up the column to give countercurrent flow. For the evaporation of water, air entering and leaving the column was tested with a wet and dry bulb thermometer from which the humidity was calculated. The exit gas for runs using carbon tetrachloride were analysed using a thermal conductivity bridge. The overall coefficients  $k_G$  were calculated from the rate of evaporation, the log mean partial pressure difference in atmospheres, and the dry surface of the discs.

Data for the evaporation of water are given in Table 1 and for the vaporisation of carbon tetrachloride in Table 2. The data are well correlated by the equation:

$$\frac{k_G P_{BM}}{3600 v \rho_m} = 0.15 \Gamma^{0.15} Re_G^{-0.4} Sc_G^{-0.5} \quad (7)$$

with a standard deviation of 8%. These data are

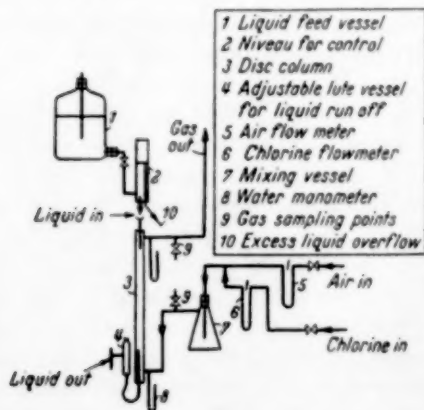


Fig. 1. The general arrangement of the experimental apparatus.

consistent with the gas film coefficients for the absorption of ammonia in water reported by STEPHENS and MORRIS. They correlated their data using a gas velocity relative to the surface velocity of the water for both co-current and counter current flow. Their data for counter current flow have been recalculated and plotted in Fig. 2. It may be seen that they agree with the vaporisation data. This correlation could have been improved by using volume rate of liquid, but the data are insufficiently accurate to depart from the usual practice.

#### Physical absorption of chlorine

Air and chlorine were passed through flowmeters and mixed in vessel 7 (Figs. 1). The gases were analysed before entering and after leaving the column. The liquor was analysed at the lute vessel. From the liquid and gas analyses the rate of absorption of chlorine was calculated and the run rejected if the calculated rate from the gas analysis differed from the rate calculated from the liquid analysis by more

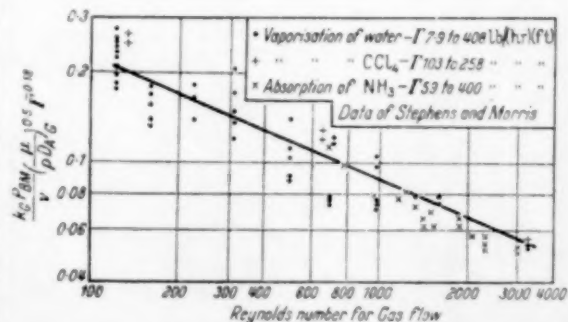


Fig. 2. The gas film coefficients for the disc column.

Table 3. Physical absorption of chlorine in carbon tetrachloride.

Run No.	Liquor			Gas			N.A.		$\Delta P$ L.m. atm.	$K_G$	$Hk' L$
	$\Gamma$ lb./ (hr.) (ft.)	$Cl_2$ conc. $10^{-3}$ lb. mol / ft. <sup>3</sup>	Temp., ° F.		$\epsilon$ f.p.s.	% $Cl_2$		Temp., ° F in			
			in	out		out	in				
1	342	4.26	86.2	73.0	2.95	6.4	7.7	83.6	1.79	1.85	0.254
2	128	5.96	74.4	68.2	0.464	6.8	11.5	73.6	0.953	0.965	0.130
3	31.1	7.45	77.6	66.0	0.582	6.5	7.9	76.2	0.270	0.310	0.0484
4	80.2	5.38	79.8	70.0	2.62	5.8	6.2	74.6	0.532	0.490	0.0950
5	74.5	5.26	76.2	67.4	0.437	5.6	7.7	73.8	0.482	0.492	0.0847
6	31.1	6.51	77.4	67.0	0.378	5.6	6.6	76.8	0.241	0.262	0.0531
7	128	6.31	74.8	68.6	0.465	7.0	11.9	73.6	0.991	1.07	0.140
8	170	4.71	76.6	72.2	0.504	6.6	10.6	75.2	0.980	0.955	0.127
9	23.0	13.4	80.6	66.2	2.10	11.3	12.1	78.8	0.375	0.430	0.0411
10	71.1	9.40	87.2	69.4	2.06	9.7	10.6	84.6	0.827	0.802	0.0792
11	362	4.20	85.2	73.2	2.94	6.2	7.6	83.6	1.86	1.92	0.276
12	266	4.90	86.2	70.0	2.96	6.6	8.0	83.2	1.60	1.92	0.226
13	63.9	5.26	81.7	65.9	1.80	5.2	5.8	78.6	0.454	0.403	0.0755
14	180	5.75	76.6	76.2	2.02	7.3	8.2	75.6	1.24	1.18	0.164

than 10%. The overall coefficients were calculated from the equation:

$$K_G = N_A \Delta P_{L.m.} / I \quad (8)$$

From the values of  $K_G$  the liquid film coefficients were calculated from equations (6) and (7).

Previous liquid film data for this column [14] were correlated using the SHERWOOD-HOLLOWAY relation [11] in the form:

$$\frac{k'_L}{D_A} = \beta Re_L^{0.7} Sc_L^{0.5} \quad (9)$$

Equation (9) indicates that a change of temperature from 65°F to 80°F should increase the liquid film coefficient nearly 20%. On this temperature range the value of the Henry's law coefficient decreases by 20% [7]. Thus the product  $Hk'_L$  should be nearly independent of temperature.

The data for physical absorption of chlorine from air by carbon tetrachloride are given in Table 3 and plotted in Fig. 3. The data may be represented by:

$$Hk'_L = 0.0041 \Gamma^{0.7} \quad (10)$$

with a standard deviation of 10%.

#### Chemical absorption of chlorine

The first series of tests were made without using the iodine catalyst at constant liquor rate  $\Gamma = 80.2 \text{ lb.}/(\text{hr.})(\text{ft.})$ . The procedure was similar to that already described except that a small quantity of 0.1 N hydrochloric acid solution was placed in the liquid run-off tube. The concentration of physically dissolved chlorine in the liquor was calculated from the concentration of chlorine in the hydrochloric acid solution and its distribution coefficient between the acid and carbon tetrachloride. This distribution coefficient for several temperatures was calculated from data reported by PERRY [9] and *International Critical Tables* [7] and was checked by making three runs without any olefin in the liquor. These experimental distribution coefficients agreed with the calculated values within the accuracy desired. The total concentration of chlorine in the liquor was determined from the decrease in the olefin concentration after sufficient time was allowed for all the chlorine to react.

There was some substitution reaction as indicated by the smell of hydrochloric acid gas from the liquor. The amount of chlorine consumed by the substitution is small and is neglected. The ratios of the amount of chlorine absorbed determined from the liquor analysis

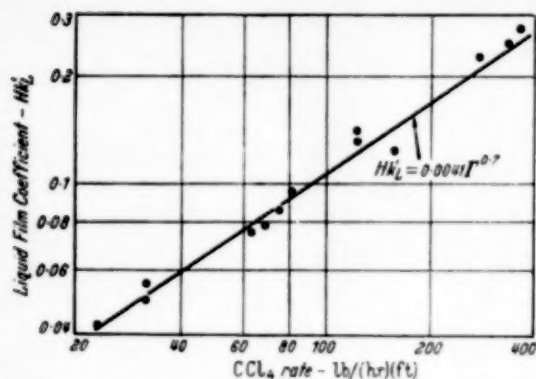


Fig. 3. The liquid film coefficients for the absorption of chlorine from air by carbon tetrachloride.

to that determined from the gas analysis are generally between 0.85 and 1.05.

With iodine in the liquor, the presence of the interhalogen compound prevented the use of the distribution method for calculating the concentration of physically dissolved chlorine in the liquor. The ratio of the physically dissolved (free) chlorine to the total amount absorbed was estimated from Fig. 4 for liquor rates of 80.2 lb./hr. (ft.), in which this ratio is plotted as a function of  $N_A/C_i$  in the absence of catalyst. The chlorine concentration at the interface,  $C_i$ , was obtained from the partial pressure at the interface required to give the observed rate of transfer through the gas film.

Tests were made at a higher liquor rate of 180 lb./hr. (ft.), and were treated in the same manner. The overall coefficient  $K_G$  and the liquid film coefficient  $k_L$  were calculated from equations (6), (7) and (8).

#### DISCUSSION OF RESULTS

The liquid film coefficients  $Hk_L$  given in Tables 4 and 5 cannot be correlated against any one

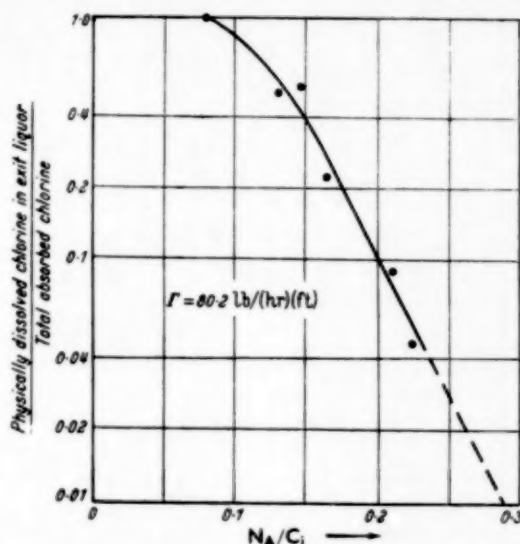


Fig. 4. The fraction of the total chlorine absorbed which is physically dissolved (in the absence of catalyst).

factor ( $C_B$ ,  $C_C$ ,  $C_i$ ,  $\Gamma$ ) independently; examination of the results shows that  $Hk_L$  increases with the olefin

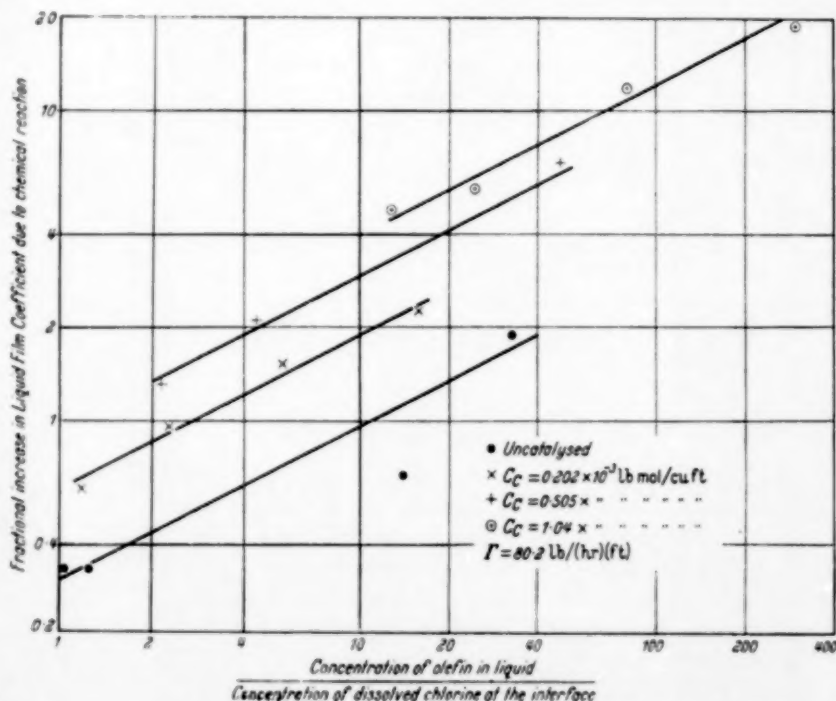


Fig. 5. Increase in liquid film coefficient due to chemical reaction.  $\Gamma = 80.2$  lb./hr. (ft.).

Table 3. Chemical absorption of chlorine in solutions of 2-ethyl 1-hexene, iodine and carbon tetrachloride  
Constant liquor rate,  $\Gamma = 80.2 \text{ lb.}/(\text{hr.})(\text{ft.})$ 

Run No.	Liquor				Gas				$10^3 C_i$	$\beta$ , ft./sec.	$10^3 N_A$		$10^3 C_e$	$\Delta P$ <i>l.m.</i>	$K_G$	$H K_L$
	Temp., °F.		$10^3 C_A$		$\% Cl_2$		<i>in</i>	<i>Liquor</i>			<i>Gas</i>					
	<i>in</i>	<i>out</i>	Free	Total	<i>out</i>	<i>in</i>										
1	79.8	70.0	5.38	5.38	0	0	5.8	0.2	0.53	0.49	0	0.436	0.0795	0.095	0.095	
2	81.2	80.0	3.28	6.54	4.68	4.68	4.6	5.8	0.64	0.70	0	0.6375	0.0931	0.116	0.116	
3	81.2	77.6	3.28	6.30	4.80	4.80	4.55	5.75	0.62	0.70	0	0.6370	0.0912	0.125	0.125	
4	82.0	71.4	0.97	4.40	3.87	3.87	2.4	2.9	0.43	0.51	0	0.4227	0.0992	0.125	0.125	
5	84.7	73.1	0.033	3.08	31.4	31.4	1.0	1.4	0.36	0.42	0	0.4118	0.167	0.256	0.256	
6	86.6	79.9	0.24	4.92	30.5	30.5	2.3	2.75	0.48	0.49	0	0.4242	0.109	0.147	0.147	
7	73.8	70.3	0.47	6.93	5.15	5.15	3.2	3.85	0.68	0.73	0	0.4332	0.112	0.146	0.146	
8	76.7	70.2	7.00	7.00	4.25	4.25	3.0	3.74	0.70	0.85	0.205	0.4318	0.119	0.158	0.158	
9	77.8	70.4	5.80	5.80	5.03	5.03	2.2	2.2	0.57	0.70	0.205	0.4250	0.135	0.188	0.188	
10	76.0	64.5	4.20	4.20	5.79	5.79	1.3	1.5	0.42	0.53	0.250	0.4140	0.164	0.249	0.249	
11	76.4	63.0	2.21	2.21	7.06	7.06	0.6	0.6	0.22	0.22	0.205	0.4060	0.197	0.333	0.333	
12	78.2	63.0	6.68	6.68	6.24	6.24	0.3	0.3	0.22	0.45	0.505	0.4040	0.304	0.826	0.826	
13	79.8	70.8	8.32	8.32	4.95	4.95	1.8	2.2	0.46	0.82	0.505	0.4040	0.304	0.826	0.826	
14	81.0	73.0	5.39	5.39	12.8	12.8	2.4	3.6	0.82	0.71	1.04	0.4040	0.304	0.826	0.826	
15	82.4	69.2	3.60	3.60	34.0	34.0	0.9	1.2	0.53	0.53	1.04	0.4040	0.304	0.826	0.826	
16	75.2	65.0	4.86	4.86	32.3	32.3	0.7	0.8	0.36	0.48	1.04	0.4040	0.304	0.826	0.826	
17	78.0	68.6	12.3	12.3	29.5	29.5	2.0	2.9	1.21	1.40	1.04	0.4040	0.304	0.826	0.826	
18	81.0	77.6	17.2	17.2	27.2	27.2	3.2	4.8	1.70	1.70	1.04	0.4040	0.304	0.826	0.826	
19	80.2	69.0	5.75	5.75	5.75	5.75	3.2	4.8	1.70	1.70	1.04	0.4040	0.304	0.826	0.826	

Table 5. Chemical absorption of chlorine in solutions of 2-ethyl hexene-1, iodine and carbon tetrachloride  
Constant liquor rate,  $\Gamma = 180 \text{ lb.}/(\text{hr.})(\text{ft.})$   
Constant air rate of 0.003 c.f.m.

Run No.	Liquor										Gas			$10^3 N_A$		$\Delta P$ <i>atm.</i>	$K_g$	$H K_L$
	Temp., °F.		$10^3 C_A$			$10^3 C_B$ <i>mean</i>	$10^3 C_i$	$10^3 C_e$	$\% C_2$		<i>Liquor</i>	<i>Gas</i>						
	<i>in</i>	<i>out</i>	<i>free</i>	<i>total</i>	<i>in</i>	<i>out</i>	<i>in</i>	<i>out</i>										
20	74.0	62.0		2.31		21.5	0.10		0.77		0.6	0.6	0.51	1.56	0.006	0.464	3.78	
21	76.0	75.6		7.75		17.9	1.21		0.77		2.0	3.4	1.72		0.027	0.346	0.92	
22	76.4	69.4		3.74		12.3	0.75		0.42		1.2	1.8	0.85	0.66	0.016	0.308	0.67	
23	77.0	74.6		6.40		11.5	1.42		0.42		2.2	3.4	1.42	1.31	0.028	0.276	0.55	
24	74.6	73.6		5.25		11.3	2.41		0		2.8	4.0	1.13	1.29	0.033	0.181	0.27	
25	75.0	66.2		0.27		12.6	0.94		0		1.1	1.5	0.47	0.44	0.013	0.108	0.31	
26	72.0	66.2		1.07		13.1	0.36		0		0.5	0.5	0.24		0.005	0.256	0.47	
27	74.8	74.2		7.70		11.8	2.44		0.42		2.8	4.6	1.70	1.90	0.037	0.250	0.46	
28	77.0	77.2		10.0		9.5	2.19		0.77		3.2	5.4	2.21	2.46	0.043	0.279	0.56	
29	76.6	72.2		5.75		0	5.40		0		7.3	8.2	1.24	1.18	0.072	0.127	0.164	



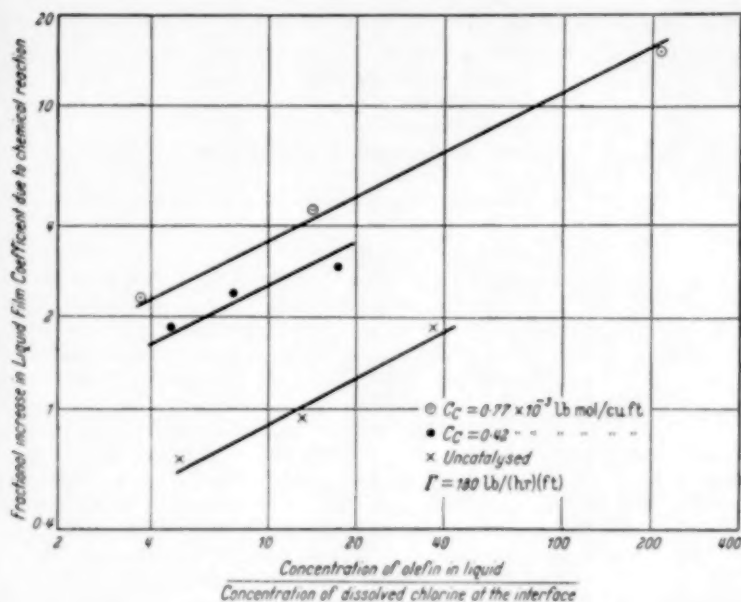


Fig. 6. Increase in liquid film coefficient due to chemical reaction.  $\Gamma = 180 \text{ lb.}/(\text{hr.})(\text{ft.})$ .

concentration, but decreases as the concentration of chlorine at the interface increases. It was therefore decided to attempt a correlation in the form used by STEPHENS and MORRIS although the latter was derived on the assumption of reaction rates infinitely fast compared with rates of diffusion, which leads theoretically to equation (5). The fractional increase in the liquid-film coefficient, by this treatment, is a function of the ratio between the concentration of dissolved reactant ( $C_B$ ) and that of dissolved chlorine at the interface.

The data of runs 1 to 19 (Table 4) are plotted in Fig. 5, and the data for runs 20 to 29 in Fig. 6. The data fall on parallel straight lines, having a slope of 0.5, the equations for which are:

$$\text{for } \Gamma = 80.2, H k_L = 0.095 [1 + (\alpha C_B/C_i)^{0.5}] \quad (11)$$

$$\text{for } \Gamma = 180, H k_L = 0.164 [1 + (\alpha C_B/C_i)^{0.5}] \quad (12)$$

The lack of correlation for the various lines is clearly due to variations of the iodine concentration. The parameter  $\alpha$  is a function of the catalyst concentration  $C_C$  and may be a function of liquor rate. When graphed in Fig. 7,  $\alpha$  is seen to vary linearly with  $C_C$ . The intercept (the value of  $\alpha$  when  $C_C = 0$ ) is

a measure of the reaction rate constant  $k_c$  in the absence of catalyst. The increase in  $\alpha$  is proportional to  $C_C$ . This result may have been anticipated because of the symmetry of  $k_c$  and  $C_B$  in the basic equation (2). Hence we may write:

$$\frac{k_L}{k'_L} - 1 = 39.2 \left[ \frac{(C_C + 0.00005) C_B}{C_i} \right]^{0.5} \\ \propto \left( \frac{k_c C_B}{C_i} \right)^{0.5} \quad (13)$$

### CONCLUSIONS

STEPHENS and MORRIS found that the increase in liquid film coefficient was proportional to the 0.83 power of the ratio  $C_B/C_i$ . In this investigation the increase is proportional to the 0.5 power of the same ratio. Equation (3) leads to the conclusion that increasing the reaction rate constant  $k_c$  would increase the exponent so that it approaches unity. However the increase in reaction

rate due to catalytic action did not alter the value of the index. It may be that the index is a function of diffusivities.

Variations in the reaction rate constant have a similar effect upon the increase in liquid film coefficient as have variations in the concentration of the liquid phase reactant.

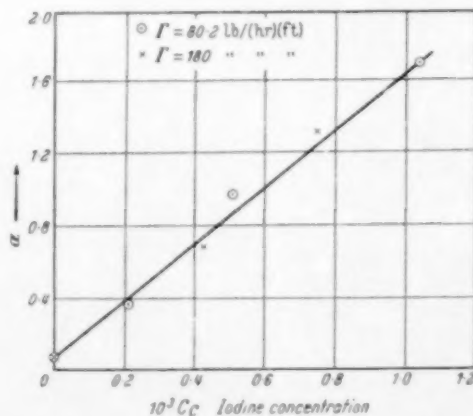


Fig. 7. The variation of  $\alpha$  as a function of iodine concentration  $C_C$ .

**Acknowledgment**—The author wishes to acknowledge the helpful advice received from Professor J. P. BAXTER.

# NOTATION

- $A$  = interfacial area, ft.<sup>2</sup>  
 $C$  = concentration of solute, lb. mol per ft.<sup>3</sup> of solution.  
 $D$  = diffusivity, ft.<sup>2</sup>/hr.  
 $H$  = Henry's law coefficient, lb. mol/(ft.<sup>3</sup>) (atm.).  
 $K$  = overall absorption coefficient.  
 $k$  = individual film coefficient.  
 $k'_L$  the liquid film coefficient for physical absorption.  
 $k_c$  = reaction rate constant, (hour)<sup>-1</sup> (lb. mol/ft.<sup>3</sup>)<sup>-1</sup>  
 $N_A$  = rate of absorption of chlorine, lb. mol/hour.  
 $P$  = pressure, atm.  
 $P_{BM}$  the logarithmic mean of the partial pressure of air at the phase boundary and in the bulk of the gas stream.  
 $\Delta P_{i,m}$  the logarithmic mean driving force, atm.  
 $Re$  = Reynolds number.  
 $Sc$  = Schmidt number.  
 $v$  = gas velocity, ft./sec.  
 $x$  = the distance of an element of the liquid film from the interface, ft.  
 $\alpha$  = a parameter defined by equations (11) and (12).  
 $\beta$  = a constant in equation (9).  
 $\Gamma$  = liquor rate, lb./(hr.) (ft.).  
 $\mu$  = absolute viscosity, lb. mass/(ft.) (hr.).  
 $\rho$  = density, lb./ft.<sup>3</sup>  
 $\rho_M$  = density of the gas stream, lb. mol per cu. ft.

# Subscripts

- $A$  = refers to chlorine.  
 $B$  = refers to 2-ethyl hexene-1.  
 $C$  = refers to iodine.  
 $G$  = refers to the gas.  
 $i$  = refers to the dissolved chlorine at the interface.  
 $L$  = refers to the liquor.

The units used are feet, hours, pounds and atmospheres.

# REFERENCES

- [1] BRUNNER, E.; Z. Phys. Chem. 1904 **47** 67. [2] COMSTOCK, C. S. and DODGE, B. F.; Ind. Eng. Chem. 1937 **29** 520. [3] CRYDER, D. S. and MALONEY, J. O.; Trans. Amer. Inst. Chem. Engrs. 1941 **37** 827. [4] DANCKWERTS, P. V.; Trans. Faraday Soc. 1950 **46** 300. [5] HARTE, C. R. and BAKER, E. M.; Ind. Eng. Chem. 1933 **25** 1128. [6] HITCHCOCK, L. B.; Ind. Eng. Chem. 1934 **26** 1157; 1937 **29** 302. [7] International Critical Tables 1928, 1st edn., Vol. III 261 McGraw-Hill, New York. [8] JENNY, J. H.; Thesis in Chem. Engrg., M.I.T., 1936, as reported by SHERWOOD [12]. [9] PERRY, J. H.; Chemical Engineers' Handbook 1950 3rd edn. 3d. 674, McGraw-Hill, New York. [10] RIGGLE, J. W. and TEPE, J. B.; Ind. Eng. Chem. 1950 **42** 1036. [11] SHERWOOD, T. K. and HOLLOWAY, F. A. L.; Trans. Amer. Inst. Chem. Engrs. 1940 **36** 39. [12] SHERWOOD, T. K.; Absorption and Extraction 1937 1st edn. McGraw-Hill, New York. [13] SPECTOR, N. A. and DODGE, B. F.; Trans. Amer. Inst. Chem. Engrs. 1946 **42** 827. [14] STEPHENS, E. J. and MORRIS, G. A.; Chem. Eng. Progress, 1951 **47** 232. [15] WHITMAN, W. G.; Chem. Metall. Eng. 1923 No. 4 146. [16] WILLIAMSON, R. V. and MATHEWS, J. H.; Ind. Eng. Chem. 1924 **16** 1157.

VOL.  
2  
1953

## The kinetics of the addition of chlorine to olefins in carbon tetrachloride

G. H. ROPER

School of Chemical Engineering, N.S.W. University of Technology, Broadway, N.S.W.

(Received 16 January 1953)

**Summary**—For the interpretation of the rates of absorption of chlorine from air by solutions of olefins and iodine in carbon tetrachloride, it is necessary to know the kinetics of the addition of chlorine to the olefins under the conditions of the absorption. The rate of addition of chlorine to 2-ethyl hexene-1 and to oleic acid in carbon tetrachloride was found proportional to the concentration of the chlorine and to the concentration of the olefin. With excess cyclohexene, the rate of addition of chlorine to cyclohexene in carbon tetrachloride was found to be proportional to the second power of the chlorine concentration and independent of the concentration of cyclohexene.

**Résumé**—Pour interpréter la cinétique du lavage des mélanges chlore-air avec des solutions dans  $\text{CCl}_4$ , d'oléfines et d'iode, il est indispensable de connaître la cinétique de l'addition du chlore aux oléfines dans les mêmes conditions.

La vitesse d'addition du chlore à l'ethyl-2 hexène-1 et à l'acide oléique dissous dans  $\text{CCl}_4$  est proportionnelle à la concentration du chlore et à celle de l'oléfine. Dans la cas du cyclohexène, la vitesse d'addition est proportionnelle au carré de la concentration du chlore et indépendante de celle du cyclohexène, si ce dernier reste toujours en excès par rapport au chlore absorbé.

### INTRODUCTION

In a previous publication [1] the rates of absorption of chlorine from air by solutions of 2-ethyl hexene-1 in carbon tetrachloride were reported. The rate of reaction between chlorine and 2-ethyl hexene-1 in solution appreciably affects the rate of absorption, and in order to interpret the results of the absorption experiments it is necessary to know the kinetics of this addition. This paper describes the investigation into the kinetics of this addition, as well as the addition of chlorine to oleic acid and cyclohexene under similar conditions. The rates of absorption of chlorine into solutions of these olefins is at present being studied.

The addition of halogens to olefins in non-polar solvents has been reviewed by DE LA MARE [2] and by REMICK [3]. Both agree that the additions are difficult to reproduce and that the kinetics are often intractable. The rate of addition is increased by polar molecules—such as hydrogen bromide and water—and is decreased by oxygen. The rates of addition which are sufficient to influence considerably the rates of absorption are much faster than the rates of reaction in solution which have been previously measured.

The rates of addition studied in this paper are so great that the usual unsteady-state method of

measurement is unsuitable. A steady-state method is required. HOUGEN and WATSON [4] give a mathematical treatment of flow reactions for the cases when the stream of reactants moves progressively through the reactor without longitudinal mixing and without appreciable mixing in the direction of flow. These conditions are satisfied in a tubular reactor. HOUGEN and WATSON give the reaction volume,  $V$ , for a specified conversion,  $x$ , for a constant mass feed rate,  $F$ , as

$$\frac{V}{F} = \int_0^x \frac{dx}{r}$$

where  $r$  is the rate of reaction, moles of component  $A$  converted per unit volume of the reacting system per unit time. For a reacting system, the density of which is independent of the conversion  $x$ , the particular solution for the specific reaction rate,  $k_a$ , for a second-order irreversible reaction is

$$k_a = \frac{F}{V\rho(c_{B0} - c_{A0})} \ln \frac{c_{A0}c_B}{c_{B0}c_A} \quad (1)$$

or, for equal concentrations of the reactants,

$$k_a = \frac{F}{V\rho} \frac{(c_{A0} - c_A)}{c_{A0}c_A} \quad (2)$$

## EXPERIMENTAL APPARATUS AND PROCEDURE

The general arrangement of the apparatus is shown in Fig. 1, and the details of the glass tubular reactors. The left-hand liquid feed vessel held a solution of an

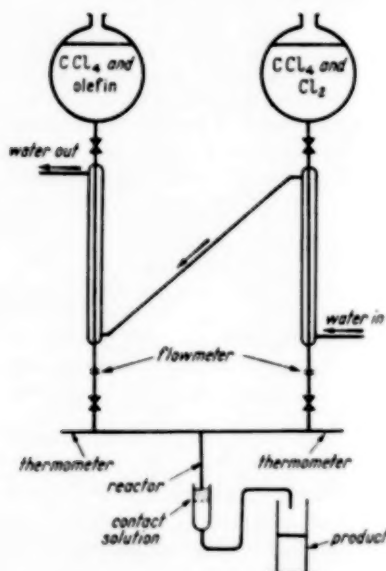


Fig. 1. The general arrangement of the apparatus.

olefin in carbon tetrachloride. The liquor from each vessel passed downwards through a flowmeter and

Table 1. The dimensions of the glass tubular reactors

Reactor No.	1	2	3	4	5
Length, cm	22.9	11.4	6.8	15.3	8.0
Diameter, cm	0.249	0.267	0.280	0.122	0.124
Volume, ml	1.116	0.637	0.418	0.180	0.096

entered the reactor, a glass tee, from opposite sides. The reacting mixture passed downwards from the tee through a contact solution (5 normal hydrochloric acid) to a product receiving vessel. For each run a mass balance was calculated from the analyses of the liquor in each of the liquid feed vessels, the rate of feed from each vessel, the analysis of the product, and the total liquor rate. If the balance was more than 6% out, the run was rejected. The initial concentration of a reactant, i.e.  $c_{40}$  (chlorine) or

$c_{80}$  (olefin), was calculated from its concentration in a liquid feed vessel, and the fraction of the total liquor rate contributed from this vessel. The concentration of chlorine in the discharge from the reactor was calculated from its concentration in the contact solution and a distribution coefficient for chlorine between carbon tetrachloride and 5 normal hydrochloric acid. The distribution coefficient was determined as a function of temperature by running only liquid from the right-hand feed tank (i.e. without olefin) and determining the concentration in both phases. The value of  $V$  used in equations (1) and (2) allowed for one-half of the volume of the liquid stream as it passed through the contact solution assuming that the stream cross-section remained constant during this period. Thus all the variables appearing in equations (1) and (2) were known.

Because of the possible effects of water and oxygen, the solutions were made from carbon tetrachloride saturated with both water and air. The addition was carried out in the dark.

## Reaction Products

Analysis of the reaction products showed that there was no hydrogen chloride formed, indicating that no substitution was taking place. Within the limits of accuracy of the analyses, one mole of chlorine reacted with one mole of olefin.

## Materials

The carbon tetrachloride was purchased from Imperial Chemical Industries of Aust. and New Zealand Ltd. of Botany, and was labelled "sulphur-free." It was redistilled in a glass laboratory still, the column of which contained twelve theoretical plates, at a reflux ratio greater than 10 : 1. The first and last 10% of the distillate was discarded. As collected and used, the carbon tetrachloride conformed to the following tests of the British Pharmacopoeia: boiling point, specific gravity, and the limit tests for ionisable chlorides and free chlorine.

The 2-ethyl hexene-1 was prepared from 2-ethyl hexanol and sulphuric acid. The 2-ethyl hexene-1 as used conformed to the following tests:

1. Boiling point, 120–121°C.
2. Specific gravity (15°C/15°C), 0.715–0.717.
3. Iodine number 225, corresponding to a purity of 99.5%.



- When 10 ml were shaken with 10 ml of water, and allowed to separate, the aqueous layer was neutral to litmus, indicating no free acid or alkali.

The oleic acid was obtained from *New South Wales Government Stores* and conformed to the requirements of the British Pharmacopoeia.

The cyclohexene was prepared from cyclohexanol and phosphoric acid. The cyclohexene as used conformed to the following tests :

- Boiling point, 82.8–83.6°C.
- Specific gravity (20°C/4°C), 0.812.
- Iodine number 306, corresponding to a purity of 99.0%.
- No free acid or free alkali.

The chlorine was supplied by *I.C.I.A.N.Z.* of Botany in steel cylinders. It was not less than 99.5% as Cl. It was used as received.

## RESULTS AND DISCUSSION

### The Addition of Chlorine to 2-Ethyl Hexene-1

The first reaction chosen for study was between chlorine and 2-ethyl hexene-1 in carbon tetrachloride. In all the runs, the initial concentration of the olefin ( $c_{B0}$ ) exceed the initial concentration of the chlorine ( $c_{A0}$ ) because this condition corresponds to the conditions during the gas absorption experiments. The data from the rate measurements are given in Table 2.

The temperatures at which the rates were measured fall into three groups – nine measurements at 19.4°C to 22.8°C, six measurements at 37.8°C to 38.9°C, and ten measurements at 12.8°C to 13.9°C. The calculated values of the specific reaction rate within each group is satisfactorily constant when calculated from equation (1). The reaction is thus second-order, its kinetics being expressed by

$$-\frac{dc_A}{dt} = k_a c_A c_B \quad (3)$$

The data from Table 2 has been grouped according to temperature to give the following average results.

Temperature, °C	$k_a$
21	152
38	173
13	132

The activation energy calculated from these grouped

results is 2,000 cal. per g. mole. The effect of temperature on the specific reaction rate is approximately the same as its influence on the diffusivities of the reacting molecules.

### The Addition of Chlorine to Oleic acid

The rate of this addition was measured in the same manner as the rate of addition of chlorine to 2-ethyl hexene-1. The data for these measurements are given

Table 2. The addition of chlorine to 2-ethyl hexene-1

Run No.	Temp. °C	$c_{A0}$	$c_{B0}$	$c_A$	$V_p/F$ sec.	$k_a$
1	19.4	0.0091	0.0209	0.0023	0.600	152
2	19.4	0.0091	0.0209	0.0032	0.376	161
3	19.4	0.0091	0.0209	0.0045	0.284	136
4	21.1	0.0110	0.0211	0.0034	0.325	139
5	21.1	0.0110	0.0211	0.0046	0.324	180
6	21.1	0.0110	0.0211	0.0059	0.232	157
7	22.8	0.0160	0.0194	0.0056	0.618	136
8	22.8	0.0160	0.0194	0.0068	0.376	168
9	22.8	0.0160	0.0194	0.0092	0.259	143
10	38.3	0.0165	0.0228	0.0045	0.586	150
11	37.8	0.0165	0.0228	0.0060	0.358	180
12	38.9	0.0165	0.0228	0.0072	0.257	190
13	38.3	0.0143	0.0242	0.0059	0.241	188
14	37.8	0.0143	0.0242	0.0052	0.339	158
15	38.3	0.0143	0.0242	0.0040	0.548	163
16	13.9	0.0189	0.0242	0.0059	0.579	128
17	13.9	0.0189	0.0242	0.0079	0.363	141
18	13.9	0.0189	0.0242	0.0095	0.251	150
19	13.9	0.0189	0.0242	0.0153	0.094	121
20	13.9	0.0189	0.0242	0.0170	0.054	132
21	12.8	0.0208	0.0242	0.0181	0.054	115
22	12.8	0.0208	0.0242	0.0162	0.093	114
23	12.8	0.0186	0.0242	0.0097	0.258	130
24	12.8	0.0186	0.0242	0.0072	0.350	156
25	12.8	0.0186	0.0242	0.0056	0.573	135

in Table 3. The temperatures at which the rates were measured fall into two groups – five measurements at 19.4°C to 23.3°C, and five measurements at 40.0°C. to 42.2°C. The calculated values of the specific reaction rate in each group is satisfactorily constant; the reaction is therefore second-order, its kinetics being expressed by equation (3). The values of the specific reaction rates for the addition of chlorine to oleic acid are the same, within the limits of error of the method, as the values obtained for the specific

reaction rate for the addition of chlorine to 2-ethyl hexene-1.

Table 3. The addition of chlorine to oleic acid

Run No.	Temp. °C	$c_{A0}$	$c_{B0}$	$c_A$	$V_p/F$ sec.	$k_a$
1	29.6	0.0071	0.0458	0.0030	0.130	153
2	19.4	0.0076	0.0268	0.0033	0.212	162
3	22.2	0.0205	0.0259	0.0038	0.695	170
4	23.3	0.0124	0.0350	0.0014	0.570	140
5	23.3	0.0186	0.0282	0.0020	0.826	169
6	40.6	0.0091	0.0170	0.0018	0.682	195
7	40.0	0.0064	0.0183	0.0015	0.504	191
8	40.0	0.0064	0.0183	0.0023	0.324	200
9	41.9	0.0064	0.0183	0.0036	0.169	199
10	42.2	0.0064	0.0183	0.0042	0.103	176

The data from Table 3 has been grouped according to temperature to give the following average results :

Temperature, °C	$k_a$
22	159
41	192

The activation energy is the same as that of the addition to 2-ethyl hexene-1 within the limits of error of the method.

#### The Addition of Chlorine to Cyclohexene

The measurements of the rates of addition were carried out under the same conditions. The data is given in Table 4. The temperatures at which the rates were measured fall into three groups - eight measurements at 26.7°C to 27.8°C, five measurements at 18.9°C, to 21.1°C, and five measurements at 35.0°C, to 37.8°C. The calculated values of the specific reaction rate using equation (1) vary greatly. That the reaction product has no influence on the rate of addition is shown by run 8, to the feed of which was added sufficient 1, 2-dichlorocyclohexene to give an initial concentration of 0.130 g. moles per litre. In runs 12 and 13, the initial concentration of the cyclohexene was 0.0910 g. moles per litre, a concentration considerably higher than used in the other runs. The specific reaction rate,  $k_a$ , is correspondingly low. It is possible that the reaction is zero order in respect to the cyclohexene. Specific

reaction rates were calculated, for zero order in respect to the olefin, assuming that the rate was first, second, or third order in respect to the chlorine concentration. The calculated values of the specific reaction rate were most nearly constant for the assumption of second order in respect to the chlorine concentration and zero order in respect to the cyclohexene concentration. The variation in this specific reaction rate,  $k_b$ , is rather greater than the variations previously obtained for  $k_a$  (i.e. for 2-ethyl hexene and oleic acid). The kinetics for the reaction may be expressed by

$$-\frac{dc_A}{dt} = k_b c_A^2 \quad (4)$$

The data from Table 4 has been grouped according to temperature to give the following average results :

Table 4. The addition of chlorine to cyclohexene

Run No.	Temp. °C	$c_{A0}$	$c_{B0}$	$c_A$	$V_p/F$ sec.	$k_a$	$k_b$
1	26.7	0.0075	0.0341	0.0025	0.547	65	500
2	27.2	0.0110	0.0302	0.0032	0.293	182	755
3	27.8	0.0138	0.0268	0.0063	0.102	336	845
4	26.1	0.0051	0.0225	0.0017	0.568	93	690
5	26.7	0.0059	0.0212	0.0028	0.248	150	770
6	26.7	0.0122	0.0167	0.0055	0.161	390	620
7	26.7	0.0118	0.0170	0.0051	0.148	435	750
8	27.8	0.0147	0.0185	0.0051	0.197	430	650
9	21.1	0.0055	0.0292	0.0014	0.875	91	610
10	21.1	0.0074	0.0201	0.0018	0.721	118	590
11	21.1	0.0074	0.0201	0.0017	0.839	108	550
12	18.9	0.0112	0.0910	0.0042	0.297	38	500
13	19.4	0.0112	0.0910	0.0013	1.49	17	480
14	35.0	0.0062	0.0168	0.0034	0.147		900
15	35.0	0.0067	0.0159	0.0012	0.805		850
16	36.1	0.0069	0.0156	0.0011	0.832		920
17	37.8	0.0045	0.0202	0.0027	0.187		790
18	37.2	0.0070	0.0178	0.0016	0.670		740

Temperature, °C	$k_b$
27	700
20	550
36	840

From the data, the activation energy is 2,000 cal. per g. mole, the figure obtained for the two previous reactions.

Some independent evidence is available to confirm the finding that the rate of addition of chlorine to cyclohexene is zero order in regard to the concentration of the olefin. The rate of absorption of chlorine by solutions of 2-ethyl hexene-1 is increased by increasing the concentration of olefin in the liquor. Preliminary tests have indicated that oleic acid has a similar influence on the rate of absorption of chlorine, but that the rate of absorption of chlorine is not increased by increasing the concentration of cyclohexene in the liquor, provided that there is sufficient cyclohexene in the liquor to react with all the chlorine absorbed.

## ACKNOWLEDGMENTS

The author wishes to express his indebtedness to Dr. G. K. W. CAVILL and Professors BAXTER and NYHOLM for discussions during the progress of this work.

## NOTATION

$c_A$	= the concentration of chlorine in the discharge from the reactor	g moles per litre
$c_{A0}$	= the concentration of chlorine in the feed to the reactor	g moles per litre
$c_B$	= the concentration of olefin in the discharge from the reactor	g moles per litre
$c_{B0}$	= the concentration of olefin in the feed to the reactor	g moles per litre
$F$	= the total liquor feed rate to the reactor	g per sec.
$k_a$	= the specific reaction rate, defined by equations (1), (2) and (3)	l./g mole (sec.)
$k_b$	= the specific reaction rate, defined by equation (4)	l./g mole (sec.)
$t$	= time	sec.
$\rho$	= density	g per cc

## LITERATURE CITED

- [1] ROPER, G. H.; *Chem. Eng. Sci.* 1953 **2** 18. [2] DE LA MARE, P. B. D.; *Quarterly Reviews* 1949 **3** 126. [3] REMICK, A. E.; *Electronic Interpretations of Organic Chemistry*, Chapman and Hall Ltd., London, 1941 p. 433. [4] HOUGEN, O. A. and WATSON, K. M.; *Chemical Process Principles*, John Wiley and Sons, Inc., New York (1947) p. 832.

## Overall heat flux values from condensing steam to boiling liquid

E. A. JONES and L. W. J. LOVELESS

Courtaulds Ltd., Research and Development Section, Coventry

(Received 5 October 1952)

**Summary**—From values of the overall heat transfer coefficients determined over a range of temperature differences the corresponding total heat flux values have been calculated for the system studied. The temperature difference corresponding with the maximum heat flux is deduced.

**Résumé**—L'auteur mesure le coefficient global de transmission thermique pour tout une gamme de différence de température. Il en déduit les valeurs du flux thermique total et la valeur de la différence de température correspondant au maximum de flux.

### INTRODUCTION

To check the calculated design heat exchange surface of an evaporator calandria and also to obtain some experience with the alloy steel tubes proposed, it was considered advisable to undertake some small scale tests before proceeding with the manufacture of the full scale equipment.

The proposed evaporator calandria was to be fitted with vertical 18/8/3/1 Cr/Ni/Mo/Ti stainless steel alloy tubes having an internal diameter of 1.50 inches. The small scale apparatus for carrying out the required tests was therefore designed to incorporate a length of the same type of alloy steel tube.

Apart from the mechanical performance of the alloy steel tube, which was quite satisfactory, the results obtained were of particular interest in that they clearly showed a maximum value of the total heat flux when this was plotted against the mean temperature difference between the heating and heated fluids.

### APPARATUS

A diagram of the apparatus is given in Fig. 1.

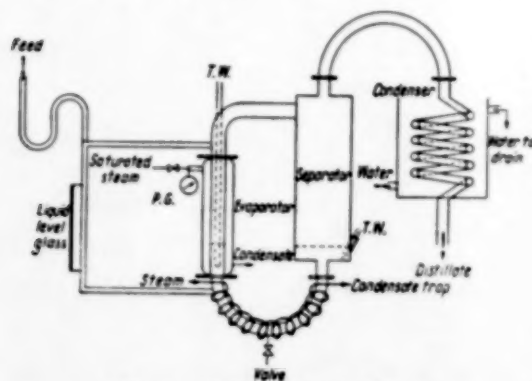


Fig. 1. Diagram of apparatus

The evaporator consisted of a vertical length of the alloy steel tube 13in. long surrounded by a 3in. diameter carbon steel steam jacket of 12in. overall length. The evaporator tube was provided with a liquid level glass into the top of which the fresh liquor feed was metered through a sealing tube. The feed liquor was introduced in this manner in order to prevent crystallisation in the level glass. The top and bottom of the evaporator tube were connected with similar alloy steel tubes of 1½in. and 1in. nominal diameters respectively to a separating chamber which was a simple vessel 18in. high and 6in. diameter also made of the same grade of alloy steel.

At the lowest point in the 1in. liquor line from the separator to the evaporator a drain valve was fitted for withdrawal of residue liquors.

Vapour from the top of the separator passed through a 1in. diameter copper pipe to a submerged-coil type condenser having four coils of 1in. diameter copper pipe each coil being 7in. in diameter. The distillate was collected from the bottom of the condenser.

A 0.5in. diameter thermowell was inserted down the centre of the evaporator tube in order to obtain the boiling temperature of the mixture. A second thermowell was installed in the separator in such a way as to indicate the liquid temperature in the bottom of this vessel.

Saturated steam was used for heating the evaporator and the pressure of this was measured by a gauge fitted as near to the evaporator steam jacket as possible. Steam was manually controlled by a needle valve.

The heat losses from the liquor return line from the separator to the evaporator were minimised by



efficient lagging and by steam tracing with a  $\frac{1}{2}$  in. diameter copper pipe carrying 30 psi gauge steam.

#### EXPERIMENTAL

The liquor under investigation consisted of a mixture of potassium acetate, acetic acid and water. An initial quantity of this liquor was put into the apparatus so that approximately one third of the evaporator tube was submerged. Heating was then commenced and as soon as proper boiling was initiated the feed liquor was introduced at a steady and metered rate.

Distilled aqueous acetic acid was collected from the

condenser while the total quantity of material in the system was maintained constant by controlled withdrawal of the residual liquor from the drain valve which had been installed for this purpose.

During the tests the thermometer in the evaporator tube gave readings which were somewhat erratic but which were generally similar to those indicated by the thermometer in the separator. Readings of the evaporator liquor temperature were therefore discontinued in favour of the separator liquor temperature.

A number of tests each of approximately three

Table 1.

Trial No.	1	2	3	4	5	6	7	8	9	10
Feed rate lbs./hour	16.2	17.6	16.5	16.5	17.4	17.3	17.4	16.5	16.0	15.1
Steam pressure psi gauge	68	71	94	91	97	96	97	100	111	123
Steam temperature °F.	315	317	334	332	336	335	336	338	345	352
Temperature of liquor from separator °F.	276	271	281	277	280	274	272	268	274	280
Mean temperature difference °F.	39	46	53	55	56	61	64	70	71	72
Distillate rate lbs./hour	3.92	4.18	4.03	4.80	4.69	5.02	5.04	4.73	4.67	4.73
Distillate composition % wt. acetic acid	10.5	10.3	10.7	11.3	11.3	11.5	11.3	11.3	11.0	11.5
Sensible heat supplied to feed Btu/hr.	2620	2790	2740	2680	2870	2780	2770	2580	2570	2490
Latent heat supplied to distillate Btu/hr.	3231	3444	3981	3862	3771	4019	4038	3782	3728	3734
Total heat transferred Btu/hr.	5851	6234	6721	6542	6641	6799	6808	6362	6298	6224
Overall heat flux Btu/hour/sq. ft.	14900	15850	17100	16620	16900	17300	17320	16200	16010	15840
Overall heat transfer coefficient Btu/hour/sq. ft./°F.	382	345	323	303	302	284	271	232	226	220

hours duration were carried out and for each test the feed temperature, temperature of the liquor leaving the separator, steam pressure and rates at which materials entered and left the system were carefully recorded.

#### CALCULATION OF RESULTS

In order to calculate the effective overall heat transfer coefficients from the condensing steam to the boiling liquid during the periods of steady evaporation, it was assumed that the total heat passing through the heat transfer area was equal to the sum of the sensible heat required to raise the temperature of the feed to the temperature of the liquor leaving the separator plus the latent heat removed in the distillate, i.e. it was assumed that the heat losses from the separator and pipes connecting it to the evaporator were negligible and that the boiling temperature of the

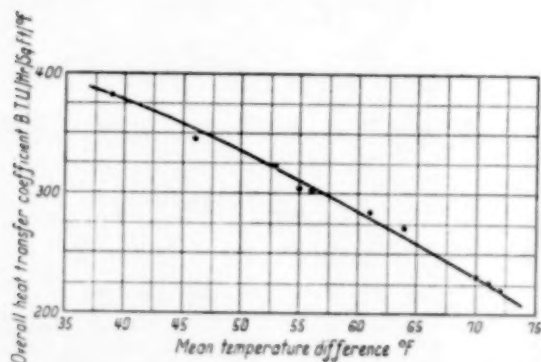


Fig. 2. Overall heat transfer coefficient vs. mean temperature difference

liquid mixture was the same as the temperature of the liquid leaving the separator. Both of these assumptions affect the quantitative accuracy of the results but, since the results from the small scale apparatus were unlikely to be identical with those obtainable in the full scale equipment, it was considered that the assumptions were justifiable and no attempt was made to determine the heat loss from the apparatus.

Data employed in calculating the effective overall heat transfer coefficients and total heat fluxes were:—

- (a) Area of heat transfer surface taken as 0.393 sq. ft.
- (b) Latent heat of acetic acid taken as 172 Btu/lb.

- (c) Average temperature of feed liquor taken as 60°F.

The averages of the experimentally observed readings together with the values of the overall heat transfer coefficients and heat fluxes calculated from them are given in Table 1. The values of the transfer coefficients and heat fluxes are plotted against the mean temperature differences in the Graphs Figs. 2 & 3.

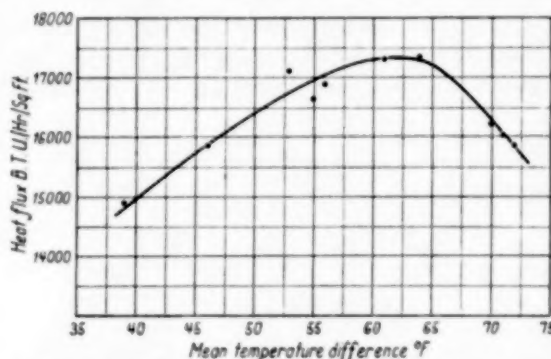


Fig. 3. Heat flux vs. mean temperature difference

#### DISCUSSION OF THE RESULTS

Figs. 2 and 3 show that the maximum heat flux value obtainable in the apparatus in which the tests were made was 17,350 Btu/hr/sq. ft. and that this occurred when the mean temperature difference was approximately 62°F. The overall heat transfer coefficient corresponding with this maximum value of the heat flux was 275 Btu/hr/sq. ft./°F.

Based on the results of these tests the most economical design of evaporator calandria for the particular service under consideration would clearly be the one utilising a mean temperature difference of approximately 62°F.

The graphs also demonstrate clearly that an increase in steam pressure, i.e. an increase in the mean temperature difference, is not necessarily synonymous with an increased rate of boiling and may in fact actually operate in the reverse direction when the mean temperature difference corresponding with maximum heat flux has been exceeded.

#### ACKNOWLEDGMENT

Acknowledgment is made to the directors of *Messrs. Courtaulds Limited* for permission to publish this paper.

## A comparative study on the rate of mixing in stirred tanks

H. KRAMERS, G. M. BAARS and W. H. KNOLL

Laboratorium voor Physische Technologie, Technical University, Delft, Netherlands

(Received 6 November 1952)

**Summary**—Measurements have been carried on the rapidity of distribution of a small amount of liquid added to the contents of an agitated vessel. With the adopted measuring method mixing speeds under different conditions can be compared. Results are given for two different tank sizes, three kinds of agitators at different locations and speeds, with and without baffles.

**Résumé**—Des mesures ont été effectuées pour déterminer la vitesse de distribution d'une faible quantité de liquide qui est ajoutée au contenu d'un réservoir muni d'un agitateur en mouvement. La méthode de mesure appliquée permet la comparaison des vitesses de mélange sous des conditions variées. Les résultats donnés portent sur deux dimensions différentes du réservoir et trois espèces d'agitateurs qui sont disposés à des endroits différents et opèrent à des vitesses variées, avec ou sans chicanes.

### 1. INTRODUCTION

Few chemical engineering operations are as evasive to experimental investigation as those connected with mechanical agitation. The choice and the design of equipment to be used for one of the many specific objectives for which agitation is required depends largely on experience. Only the power consumption of a number of standard types of agitators can be predicted within a reasonable margin thanks mainly to the work published by RUSHTON *et al.* [1].

This paper deals with batch mixing of two liquids in a cylindrical vessel which is provided with a stirring device. A fundamental approach to this particular problem would imply the measurement of the average velocity of the stirred liquid and the degree of turbulence at any place in the vessel, because essentially the problem is a hydrodynamic one. But in view of the experimental difficulties involved it is only natural that an investigation into the effect of such a flow pattern seems to be more attractive, although the results may contribute less to a general understanding of the problem.

Thus, in the present investigation the completion of the mixing process was observed by means of concentration measurements. Clearly, a complete record of the distribution of the concentration throughout the vessel as a function of time would give the most complete information on the mixing performance of the system. This again is prohibitive for practical reasons, so that we contented ourselves to measuring the concentration in two fixed points, appropriately chosen, and deriving from these an arbitrary quantity, the mixing time  $\theta$ , which is needed to obtain a certain degree of uniformity of

the mixture. The results thus obtained are of comparative interest only and no general relationships for design purposes can be expected from them. In mixing, however, even comparative data are so scarce that results of this nature may be of sufficient interest.

### 2. PRINCIPLE OF MEASUREMENT OF THE MIXING TIME $\theta$

The mixing vessel, which contains a weak electrolytic solution, is operating at the circumstances under investigation. At a certain time a small amount of a concentrated solution is thrown into the liquid. The effect of this disturbance is measured by means of two measuring cells and a record is made of the difference in concentration between those two. As the mixing proceeds the average value of this difference gradually decreases and the mixing time  $\theta$  is defined as the time interval between the injection of the disturbance and the moment from which on the measured concentration difference remains less than 0.1 per cent of the average concentration in the vessel.

WOOD, WHITTEMAN and BADGER [2] and also GEESE [3] used a somewhat similar method in their investigations into the mixing effect of paddles. A great advantage of the injection method is that the stationary flow pattern is practically not disturbed by the measurement.

### 3. EXPERIMENTAL DETAILS

The mixing experiments were carried out in two cylindrical vessels with diameters of 0.32 and 0.64 m respectively. In all cases the liquid height was equal

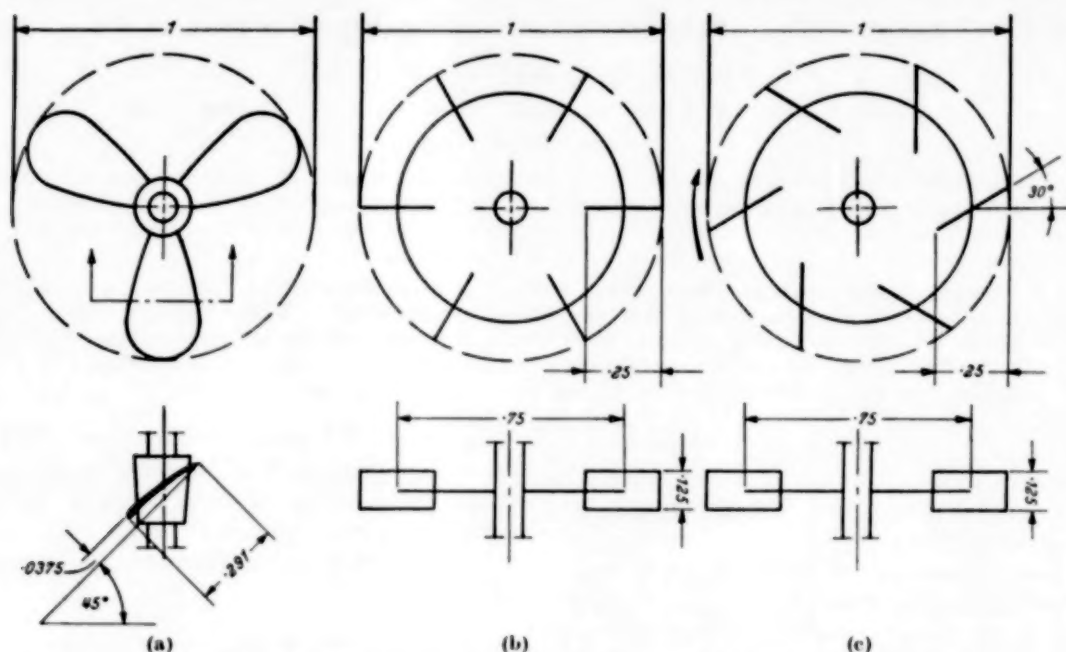


Fig. 1. Agitators used in the investigation (dimensions expressed as a fraction of the diameter  $L$ ).

to this diameter. For most of the experiments we used a 3-blade marine propeller having a diameter  $1/4$  of the tank diameter. The two propellers for the two vessels were exactly similar, their dimensions

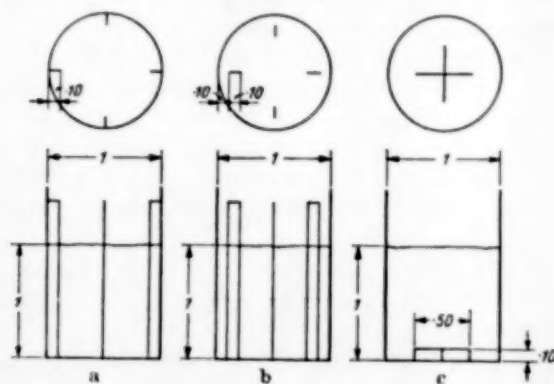


Fig. 2. Kinds of baffles investigated (dimensions expressed as a fraction of the tank diameter  $D$ ).

differing by a factor 2. Further particulars are given in Fig. 1. This figure also shows the two impeller-type agitators, which were used in the large tank only. The position of the agitator and the direction of the shaft

were variable. Its rotational speed could be varied from 300 to 2,000 r.p.m. For the large tank means were available for measuring the torque on the rotor shaft.

Either no baffles were used or one of the arrangements as shown in Fig. 2. Those of Fig. 2b have been mentioned by NEWITT [4] to produce more turbulence than the more usual arrangement of Fig. 2a. The crossed baffles on the tank bottom have been suggested by REAVELL [5] to be used with a propeller for the suspension of particles.

The injection of the strong solution was performed by mechanical means. A measured amount of solution was discharged from a small reservoir within a few tenths of a second by operating on electromagnetic shutter device. The place of injection always was half-way between the wall and the axis of the vessel, at the liquid surface. We used KCl as the dissolved electrolyte because the conductivity of its solution in water is proportional to the concentration from 1 to 20 mg/cm<sup>3</sup>.

The two similar cells for measuring the electric conductivity consisted of a few turns of Pt-wire, forming a cylinder of 25 × 25 mm, as the ground



electrode, and a Pt-wire in the axis of this cylinder as the other electrode. Both cells formed part of a Wheatstone resistance bridge in which additional compensation for capacity of the cells was possible. The 1,000 c.p.s. cross-potential was amplified, passed through a phase sensitive rectifier and fed to a fast recorder (Brush Development Co.). To protect the recorder against overload, due to relatively high output voltages occurring immediately after injection of the strong solution, the maximum amplitude of these voltages was limited by the special rectifier circuit. Fig. 3 shows a block diagram of the measuring

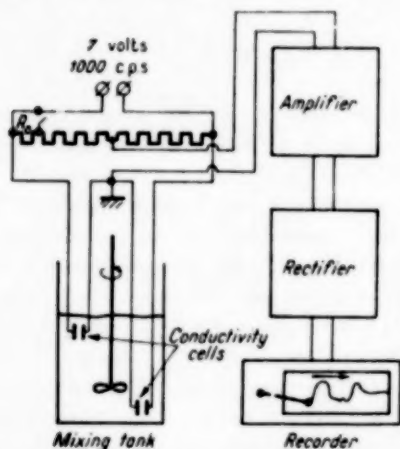


Fig. 3. Block diagram of measuring arrangement.

system. In Fig. 4 a few records are shown of the difference in electrical conductivity between the two measuring points as a function of time during a mixing experiment. Apart from this, the moment of injection was recorded and after completion of the mixing a constant deviation of 0.1 per cent of the average concentration was marked. This was achieved by short-circuiting a small part of one of the fixed resistances ( $R_0$ ) in the bridge. Fig. 4 clearly indicates how the "mixing time"  $\theta$  was read from the record taken.

The criterion for sufficient mixing at 0.1 per cent relative deviation is of course arbitrary, as well as the other measuring conditions. In order to get comparative results, the latter were standardized according to the following specifications:

Liquid in tank: tap water with 2.5 to 3 mg/cm<sup>3</sup> KCl, room temperature.

Injection liquid:  $V_{in} = 10 \text{ cm}^3$  (small tank) or  $80 \text{ cm}^3$  (large tank) with a concentration  $c_{in} = 100 \text{ mg/cm}^3$  KCl.

Size of cells: as stated above, for both tanks because for nearly sufficient mixing the dimensions of the fluctuations are large compared with the cell dimensions.

Position of cells: 1/8th of tank diameter above the bottom and under the liquid surface.

These specifications were arrived at by a great number of preliminary experiments; their significance will be treated in Section 5.

From the records in Fig. 4 it can be seen that a considerable spread in the values of  $\theta$  was to be

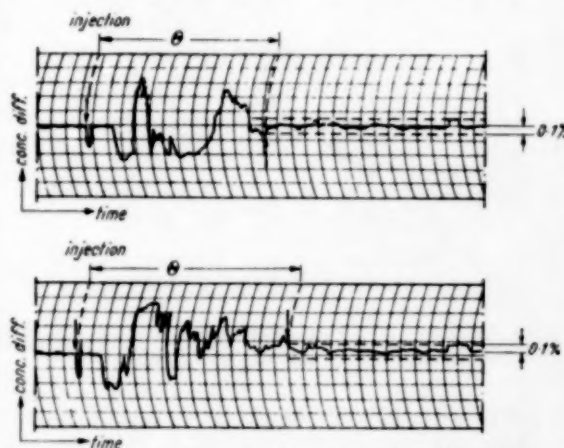


Fig. 4. Two mixing records obtained under the same circumstances, indicating how the mixing time  $\theta$  was determined.

expected, due to the fact that on a signal which is gradually decreasing to zero random fluctuations of the same order of magnitude are superimposed. From about 700 readings we found the distribution of  $\theta$  to be fairly normal with a standard deviation of about 15 per cent. We decided to repeat each measurement 15 times. Thus the average  $\theta$  values, as used for the results lie with 90 per cent probability within  $\pm 6.4$  per cent from the actual mean value. A difference of more than 10 per cent between two  $\theta$  values can be considered to be highly significant.

#### 4. EXPERIMENTAL RESULTS

The influence of a number of variables on the arbitrarily defined mixing time  $\theta$  were investigated:

(a) rotational speed of the agitator ( $n$ );

- (b) direction of rotation, for propeller only ;  
 (c) location of the propeller and inclination of the shaft ;  
 (d) presence of baffles ;  
 (e) type of rotor.  
 (a) From 8 special runs it was found that  $\theta$  was inversely proportional to the rotational speed of the agitator. Fig. 5 gives a few examples of the results.

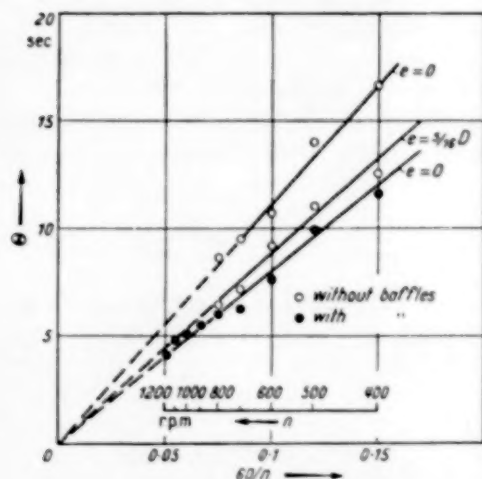


Fig. 5. Examples of proportionality between  $\theta$  and  $1/n$ ; propeller with vertical shaft, small tank.

In all these cases the product  $n\theta$  appeared to be constant well within  $\pm 10$  per cent. Subsequently all measurements under conditions (b) to (e) inclusive

were taken at only two values of  $n$ , as much different as possible. A statistical analysis of these measurements confirmed the conclusion given above. Thus it was possible to express the efficiency of mixing in terms of the product  $n\theta$ . For this we took the number of revolutions  $N$  for "sufficient mixing" under the standard conditions mentioned above. Since  $\theta$  is expressed in sec and  $n$  in rev/min, we have

$$N = n\theta/60.$$

All experiments were carried out in the flow region  $45,000 < Re < 200,000$ , where Reynolds number is defined in the usual way:

$$Re = \frac{nL^2}{60\nu}.$$

So the constancy of  $N$  for a given geometrical configuration has only been established between those limits. It is likely, however, that also for higher Reynolds numbers  $N$  will remain constant, because for these high speed agitators turbulence has nearly fully been developed in the neighbourhood of  $Re=10^4$ . This can be deduced from the measurements of RUSHTON *et al.* [1] who showed that from that Reynolds' value on the power number  $N_p$  changes only little, at least for turbines and propellers in baffled tanks.

(b) The measurements in the small tank were taken for both directions of rotation of the propeller which was always located in the lower half of the liquid. Neither appreciable, nor systematic differences between the two cases were found. From the obtained

Table 1

Number of revolutions  $N$  for sufficient mixing. Marine propeller  $L = D/4$ , vertical shaft, no baffles, both tanks.

$e/h$	$D/4$	$3D/8$	$D/2$	Tank size
0	133 —	121 177	130 176 <sup>(1)</sup>	small large
$D/8$	182 218	121 161	117 142 <sup>(2)</sup>	small large
$D/4$	157 145	135 140	92 110 <sup>(3)</sup>	small large
$5D/16$	112 —	92 —	90 —	small large

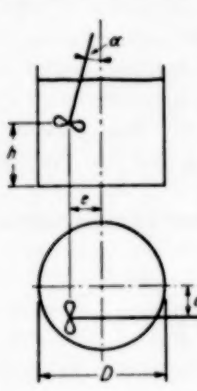
<sup>(1)</sup>Power number  $N_p = 0.26$ .

<sup>(2)</sup> $N_p = 0.34$ .

<sup>(3)</sup> $N_p = 0.36$ .

Table 2

Number of revolutions  $N$  for sufficient mixing. Marine propeller  $L = D/4$ , inclined position,  $h = D/2$ ,  $e = D/4$ , no baffles, both tanks.

	$\alpha$	$e'$	$N$	tank size
	30°	0	80	small
	30°	0	89	large
	30°	$D/4$	110	large
	15°	0	94	large
	15°	$D/4$	110	large

data, for which we refer to [6], we concluded that in general a downward thrust of the propeller was to be preferred. The data given below only apply to the latter case.

(c) Table 1 presents the final results for the propeller with a vertical shaft in a vessel without baffles. The main object of excentric location is the improvement of the pumping action of the propeller by reducing the intensity of the tangential swirl of the liquid. The results show that a sufficient excentricity considerably improves the mixing performance provided the propeller is not too near the bottom of the tank. A small excentricity, however, and a short distance between the propeller and the bottom appear to be unfavourable (e.g.  $e = D/8$  and  $h = D/4$ ), even compared with the case of a central shaft.

Table 3

Number of revolutions  $N$  for sufficient mixing.

Marine propeller on central vertical shaft,  $L = D/4$ , various kinds of baffles, both tanks.

baffles Fig.	$h =$			tank size
	$D/4$	$3D/8$	$D/2$	
2a	93	90	91	small
2a	—	100	92	large
2b	—	119	103	large
2c	107	175	140	small

Only few measurements have been made with an inclined shaft. Table 2 gives the results which show no great variations.

(d) The influence of baffles on the performance of a central propeller (Table 3) is similar to that of excentric location. It appears to be more favourable to have vertical baffles against the wall (Fig. 2a) than some distance from the wall (Fig. 2b). The crossed baffles on the bottom (Fig. 2c) are only effective for mixing if the propeller is placed immediately above it.

(e) Table 4 shows two interesting features. The first is that the agitator models Fig. 2b and Fig. 2c can give as rapid mixing as a propeller, but that the power consumption under the same conditions is of

Table 4

Number of revolutions  $N$  for sufficient mixing and power number  $N_p$ . Influence of difference rotor types on central vertical shaft,  $L = D/4$ , without and with baffles, large tank.

rotor Fig.	baffles Fig.	$h =$			$N_p$ for $h = D/2$
		$D/4$	$3D/8$	$D/2$	
1a	—	—	177	176	0.26
1a	2a	—	100	92	0.40
1a	2b	—	119	103	—
1b	2a	113	118	140	2.7
1b	2b	75	80	86	—
1c	2b	63	—	65	4.7

the order of ten times greater. In the second place, with these turbine agitators it is profitable to shift the vertical baffles towards the central axis. We did not try to find the optimum baffling conditions for these agitators.

The limitations of the measuring method and the variety of the experimental conditions make a general discussion of these results impossible. We will add only a few remarks on

- (f) vortex formation;
- (g) power consumption;
- (h) size enlargement.

(f) A central propeller mixer in a non-baffled tank works under unfavourable conditions because of the tangential swirl of the liquid which is only checked to some extent by the tank wall. At a certain speed of revolution ( $n_{\max}$ ) of the propeller it starts drawing air and its pumping efficiency sharply diminishes.

For the small tank without baffles  $n_{\max}$  was measured as a function of the propeller excentricity (Table 5).

Table 5

Approximate maximum rotor speed  $n_{\max}$ , propeller with vertical shaft,  $h = D/4$ , small tank, no baffles.

$e$	0	$D/8$	$D/4$	$5D/16$
$n_{\max}$ (rev./min.)	800	700	1200	800

It is to be noted that a small excentricity ( $e = D/8$ ) increases the tendency towards vortex formation. It also involves a greater value of  $N$  (compare Table 1).

From similar data, which will not be reported here because of their qualitative nature, we obtained the impression that as a general rule a flow pattern which shows vortex formation at the liquid surface corresponds with a relatively low mixing rate. This statement cannot be reversed, however.

(g) For several combinations in the large tank the torque exerted on the agitator shaft was measured with a dynamometer. From this the power consumption  $P$  of the agitator could be calculated, from which the dimensionless power number  $N_p$  was derived:

$$N_p = \frac{P}{\rho L^3 (n/60)^3}$$

In the range of experimental conditions,  $40,000 < Re < 100,000$ ,  $N_p$  was found to be independent of Reynolds number. The  $N_p$  values observed have been added to Tables 1 and 4. As far as a comparison with RUSHTON's data [1] permits, they agree well with these. The relatively heavy power demand of the turbine models according to Figs. 1b and 1c for obtaining about the same mixing performance as obtained with a propeller has already been mentioned in (e).

(h) The two sizes of equipment were chosen in order to see whether mixing times for large scale equipment could be predicted from smaller scale experiments. Comparison of geometrically similar cases (Tables 1, 2 and 3) shows that  $N$  remains of the same order of magnitude as long as the tendency to form a vortex is small (by excentricity or baffles). Restricting ourselves to this condition we may calculate the total energy required for sufficient mixing:

$$P \theta = N_p N \rho L^3 (n/60)^2.$$

Since both  $N_p$  and  $N$  are independent of  $Re$  for great Reynolds numbers and in the absence of vortices gravity forces do not play a part, we are led to the conclusion that in scaling up we have:

$$P \theta = \text{constant} \times \rho L^3 n^2.$$

Or for the mixing energy per unit volume:

$$\frac{P \theta}{L^3} \sim (nL)^2.$$

This means that for geometrical similarity, where the linear velocity of the agitator tips and the liquid density are kept constant, also the total mixing energy per unit volume would remain constant. Under these conditions the mixing time  $\theta$  would be proportional to the linear dimension  $L$ .

This general and somewhat tentative conclusion is not valid for those cases where vortex formation in the liquid surface is observed. From Table 1 it can be seen that for a central and slightly excentric propeller in a tank without baffles  $N$  appreciably increases with increasing diameter. Apparently not only Reynolds number must be regarded to be characteristic of the flow conditions, but also Froude number ( $Fr = g/L (n/60)^2$ ), which quantity accounts for the influence of gravitational forces. It is to be noted



that for this case also  $N_p$  depends on both  $Re$  and  $Fr$  [1]. The experimental results are too scarce however to warrant any general conclusions for this flow condition.

#### 5. SIGNIFICANCE OF THE MEASURED "MIXING TIME" $\theta$

As  $\theta$  has only been arbitrarily defined it is of interest to know whether the general results depend in some way on the chosen conditions of measurement. Apart from the operating conditions the following factors are of influence on the measured mixing time:

- (h) size and location of the measuring cells;
- (i) salt concentration of the liquid in the tank;
- (j) salt concentration and amount of injected liquid;
- (k) criterion for sufficient mixing.

(h) No experiments were performed with different sizes of measuring cells. With the adopted size not only long range concentration differences but also fluctuations of the concentrations were recorded. The great number of repetitions of a measurement can be regarded as an averaging process of the latter fluctuations.

As to the location of the cells, the applied measuring method has only significance if there is no correlation between the concentrations in the two places of measurement. Further, from observations with one cell only it was found that completion of the mixing is first reached in the immediate surroundings of the agitator. As the mixing proceeds this homogeneous region expands and finally contains the whole contents of the vessel. So in order not to find too short mixing times the cells had to be placed as far apart as practically possible.

(i) The measurements of resistances with a Wheatstone bridge involve that concentration differences can only be measured relative to the average concentration in the vessel. All other conditions remaining constant, one would find a longer mixing time for a low tank concentration than for a high one. This was verified in a number of experiments, on account of which the most convenient concentration interval of the tank liquid was chosen.

(j) The mixing times reported were found by introducing a standard disturbance ( $c_{is}$  and  $V_{is}$ ) at the liquid surface. In order to see whether the same relative results could be obtained for other conditions

of injection, for a few mixing conditions both the concentration ( $c_i$ ) and the volume ( $V_i$ ) of the injected liquid were varied. Table 6 shows the experimental results obtained in the small tank. They have been plotted on a semi-logarithmic scale in Fig. 6 which also contains a few similar data for the large tank.

Table 6

Number of revolutions  $N$  for sufficient mixing. Variation of concentration ( $c_i$ ) and amount ( $V_i$ ) of injected liquid, other measuring conditions being according to standards.

$c_i$ (mg/cm <sup>3</sup> )	$V_i$ (cm <sup>3</sup> )	$\frac{c_i V_i}{c_{is} V_{is}}$	Mixing conditions <sup>(3)</sup>		
			1	2	3
20	5	0.1	49	28	—
40	5	0.2	69	47	52
20	10	0.2	66	42	52
80	5	0.4	104	56	68
40	10	0.4	104	57	71
20	20	0.4	96	52	70
80	10	0.8	119	67	87
40	20	0.8	114	67	86
200	5	1.0	—	77	93
100 <sup>(1)</sup>	16 <sup>(2)</sup>	1.0	121	79	90
50	20	1.0	—	73	90
80	20	1.6	160	83	94
100	20	2.0	163	85	100
125	20	2.5	171	92	106
200	20	4.0	190	—	—

(1) =  $c_{is}$

(2) =  $V_{is}$

(3) see Fig. 6

It appears that  $c_i$  and  $V_i$  do not independently influence the mixing time, but only their product which is equal to the amount of salt added to the contents of the vessel. This is what one would expect provided  $c_i$  is high with respect to the average concentration in the tank and  $V_i$  small compared with the volume of the tank. Further Fig. 6 shows that  $N$  is proportional to  $\log(c_i V_i)$ , the straight lines approximately intersecting near  $N = 0$ . This means that a different choice of standard disturbance, at least within the region investigated, would not have altered our comparative results as to the mixing performance under different conditions of agitation. Finally it can be seen that the slope of the straight lines in Fig. 6 are indicative of the rapidity of mixing as well as the values of  $N$  at one standard condition of measurement. However, from this plot it cannot

be concluded that the degree of mixing increases exponentially with time.

(k) If one changes the criterion for sufficient mixing (in all experiments 0.1 per cent deviation in concentration) other mixing times are found. The obtained records did not permit a statistical investigation into the relation between the amount of deviation and the time of mixing. From a number of separate runs it was ascertained that the same mixing time was found for a standard injection and a 0.1 per cent criterion as for the injection of twice the amount of salt with a 0.2 per cent criterion.

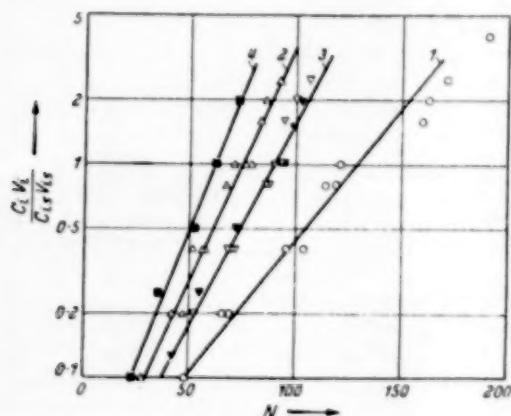


Fig. 6. Influence of the amount of injected salt on  $N$ .

1. Central propeller in small tank without baffles,  $h = 3D/8$ .
2. Eccentric propeller in small tank,  $e = D/4$ ,  $h = D/2$ .
3. Central propeller in small ( $\nabla$ ) and large ( $\blacktriangledown$ ) tank with baffles (Fig. 2a),  $h = 3D/8$ .
4. Turbine (Fig. 1c) in large tank with baffles (Fig. 2c),  $h = D/4$ .

In this section we have put forward the limitations inherent to the measuring method, at the same time

showing that the results described in the preceding section have a more general meaning provided they are considered as relative and not as absolute data.

*Acknowledgment*—We gratefully acknowledge the financial support which was given by *Het Delfts Hogeschoolfonds* for these investigations.

#### NOTATION

- $c_i$  = salt concentration of injected solution (mg/cm<sup>3</sup>).  
 $D$  = tank diameter (m).  
 $e, e'$  = eccentricity of agitator shaft (m).  
 $g$  = gravitational acceleration (m/sec<sup>2</sup>).  
 $h$  = height of agitator above tank bottom (m).  
 $L$  = diameter of agitator (m).  
 $n$  = rotational speed of agitator (rev/min.).  
 $N = \Theta/60$ , number of revolutions for sufficient mixing.  
 $P$  = power consumption of agitator (Nm/sec.).  
 $V_i$  = volume of injected solution (cm<sup>3</sup>).  
 $\Theta$  = time for sufficient mixing (sec.).  
 $\nu$  = kinematic viscosity (m<sup>2</sup>/sec.).  
 $\rho$  = liquid density (kg/m<sup>3</sup>).

$$Fr = \text{Froude number} = \frac{g}{L(n/60)^2}$$

$$N_P = \text{Power number for agitator} = \frac{P}{\rho L^3(n/60)^3}$$

$$Re = \text{Reynolds number for agitator} = \frac{nL^2}{60\nu}$$

#### REFERENCES

- [1] RUSHTON, J. H., COSTICH, E. W. and EVERETT, H. J.; Chem. Eng. Progress 1950 **46** 395, 467.
- [2] WOOD, J. C., WHITTEMORE, E. R. and BADGER, W. L.; Chem. Met. Eng. 1922 **27** 1176.
- [3] GEISE, W.; D. Zuckerind, 1933 **58** 623, 639.
- [4] NEWITT, D. M., SHIPP, G. C. and BLACK, C. R.; "Conference on mixing and agitation in liquid media," The Institution of Chemical Engineers (London) July 1951.
- [5] REAVELL, B. N.; *idem*.
- [6] KRAMERS, H. and KNOLL, W. H.; De Ingenieu, 63 1951 Ch 67.

## Book reviews

**Low Temperature Physics—Four Lectures.** By F.E. SIMON, N. KURTI, J. F. ALLEN and K. MENDELSSOHN. 132 pp. 58 illustrations. Pergamon Press Ltd., London 1952. 21s.

These lectures constituted a course given at the Royal Institution in February and March of 1950. Before publication they were revised to include some of the more recent developments, even up to 1952.

The titles of the lectures are :

Low temperature problems ; a general survey (SIMON) ;

The temperature range below 1° absolute (KURTI) ;

Liquid helium (ALLEN) ;

Superconductivity (MENDELSSOHN).

The subject dealt with is thus the phenomena occurring at extreme low temperatures (not exceeding 10° K). For the chemical engineer this field will only be of theoretical interest, since there are (as yet?) no industrial applications.

However, all those who are interested will very much enjoy the brief, simply and clearly written, and well-founded survey given of this field, which is of the utmost importance for pure physics.

P. J. HARINGHUIZEN

**J. TAYLOR : Detonation in condensed explosives.** 196 pp. + 10 plates. Oxford, Clarendon Press 1952. 25s.

L'auteur traite en 200 pages de tout ce qu'un technicien peut désirer savoir sur le phénomène de la détonation, envisagé comme un processus physico-chimique, la question des effets des détonations et de leurs applications étant en dehors du champ de l'ouvrage. Dans les cinq premiers chapitres, qui servent d'introduction, l'auteur présente, avec divers exemples et tables numériques à l'appui, des méthodes de calcul des caractéristiques des gaz engendrés par l'explosion d'un système chimique explosif donné, c'est-à-dire la composition des produits résultant de l'explosion, leur température, la pression sous laquelle ils se trouvent ; ces calculs doivent se faire en tenant compte du caractère très imparfait des gaz réels ce qui implique d'avoir à passer par les fugacités : toute la difficulté est de disposer d'une équation d'état convenable pour ce calcul des fugacités ; l'auteur a fait choix de valeurs des paramètres de cette équation, que l'on pourrait peut-être discuter mais qui conduisent à des résultats satisfaisants.

L'auteur expose ensuite la théorie classique de CHAPMAN-JOUQUET de la détonation, et son application d'abord aux explosifs ne donnant que des gaz puis à ceux, et c'est le cas des explosifs pour mines grisouteuses, dont l'explosion donne des produits solides. Des mesures expérimentales de vitesse de détonation confrontées aux calculs numériques montrent que, dans de nombreux cas, la détonation d'une cartouche cylindrique d'un explosif a lieu assez sensiblement en accord avec le schéma classique, que l'on peut appeler schéma des détonations idéales. Mais il est certains phénomènes, qui jouent d'ailleurs un rôle important dans diverses applications pratiques, qui ne peuvent se comprendre qu'en faisant appel

à des schémas plus compliqués ; ce sont la dépendance de la vitesse de détonation avec le diamètre et l'effet de confinement (nature de l'enveloppe de la cartouche) : J. TAYLOR expose les deux théories qui ont été édifiées, au cours de ces dix dernières années pour en rendre compte. Un chapitre est consacré aux deux régimes de détonation (à vitesse élevée et à vitesse faible) des explosifs liquides ou gélamineux. Enfin un dernier chapitre traite de la nature de la zone de réaction, en particulier de sa longueur et de la durée de réaction ; à cet égard, l'étude des phénomènes de détonation paraît capable d'apporter des données précieuses au physico-chimiste, dans le domaine de la cinétique des réactions non homogènes à haute température.

LOUIS MEDARD

**Physikalisches Wörterbuch.** (Two parts in one volume), (Editor: WILHELM H. WESTPHAL). Publishers: Springer Verlag. Berlin, 1952. 833 and 795 pages. DM 148 or £12 19s. 1d.

The publication of a Dictionary of Physics is an event of some importance. No such Dictionary has appeared in English since Glazebrook and none in German since the *Physikalisches Handwörterbuch* nearly twenty years ago. The present Dictionary is indeed to be regarded as a successor to the latter work, but is intended to cover a wider field, including physical chemistry, astrophysics, and to some extent geophysics and biophysics. It does not claim to cover applied physics except in so far as it is of value for pure research, being intended for the physicist who wishes to obtain information on branches of physics in which he is not a specialist or for the non-physicist who, possessing a certain amount of physical knowledge, needs information on the ideas and problems of physics.

It must be said at once that this book will prove very useful : but there are unfortunately several respects in which it falls short of the standard which it might have been expected to attain. This is particularly true of the treatment of certain aspects of modern physics, where some of the articles are clearly "second-hand" accounts. This is perhaps not surprising when one remembers the losses that German physics has suffered since 1933 and when one sees that of the 80 contributors to the Dictionary all but 6 are resident in Germany to-day. To take the subject of atomic energy, for example, there is a fairly good general description of a nuclear pile but no reference to or description of existing piles. There is a very inadequate account of neutron spectroscopy with no indication that anything can be learned about the structure of matter by neutron diffraction, let alone any reference to the results obtained. There is, too, practically no mention of an atomic bomb, certainly not under that heading. Moving farther afield, the reviewer could find no mention of antiferromagnetism, multiple beam interferometry, interference microscopy or epitaxy, to take a few subjects chosen at random ; and other subjects were not always found to be as complete or up-to-date as they might have been. For example, in an otherwise very good series of articles on valency no account is given of PAULING's

recent derivations of valencies from magnetic considerations although his 1949 Royal Society paper, which deals with his latest ideas, is actually included in the bibliography. The bibliography itself is such as to suggest that the Dictionary is intended only for German-speaking readers, as the works quoted are, wherever possible, those published in that language. In the article on the Compton effect, for example, there is no reference in the bibliography to COMPTON and ALLISON's standard work on x-rays; and in the majority of instances a translation into German or a review account in that language is preferred to an original account in another language. No bibliography at all is given in the article on biophysics, although this deals, among other things, with the effects of radiation on living matter, a subject on which there is no lack of published work.

Enough has, perhaps, been said to indicate the way in which, in many instances, the treatment of various subjects falls short of the desired standard; and it may be worth while turning our attention to the editorial aspects of the work. The editing of such a volume as that under review, a volume containing definitions of about 10,500 terms with about 1,800 diagrams, and running to over 1,600 pages, is a formidable task; and some slips or oversights are inevitable, especially in a first edition. There are, however, certain points which must be mentioned. First, all the articles are unsigned, which is a pity in the reviewer's opinion. Further, in some instances cross references are given to terms which are not given as quoted. For example, under "Absorptionsquerschnitt" reference is made to "Einfangreaktionen," but this term is not listed, and the term actually defined is "Einfangprozess." Again, the same physical concept is often defined in two or more places, and sometimes differently. For example, in the definition given under the heading "Bremsstrahlung" the term is restricted to the production of continuous x-rays in an x-ray tube, and this point of view is maintained in the article on x-rays; but in that on  $\gamma$ -rays the term is rightly extended to cover the production of x-rays by a sudden deceleration of electrons, although the author of the article seems inclined to regard the resulting radiation not as x-rays but as  $\gamma$ -rays. Another example is provided by the treatment of the electronic configurations in the heavy elements. Under the term "Actiniden" the modern view is given that the series of elements of atomic number 90 and upwards is to be considered as a "5-f" series, the elements in this series differing in the number of electrons in their 5-f shells; but in Table 11, "Schalenaufbau der Elemente," the differences appear in the 6-d shell, although the configurations are admitted to be uncertain. In this table, too, the series stops at uranium. On the other hand, a good presentation is given in Fig. 6, under "Periodisches System der Elemente." No doubt such overlapping and discrepancies are very difficult to avoid but they undoubtedly detract from the value of the work.

The Dictionary is arranged strictly alphabetically, which appears to be satisfactory. There are several appendices, consisting of conversion tables of physical units, the Periodic table, etc., tables of physical constants, a supplement to the dictionary proper, a short history of physics and a list of well-known physicists with their dates: the latter list admittedly contains mainly the names of physicists from German-speaking regions. Not a few misprints occur, but no serious ones were noted.

In spite of the faults of the Dictionary, and they are many, it can still be said that it is a valuable book. The reviewer, for one, is glad to have it on his shelves. J. THEWELIS

**BRUNO RIEDIGER; Berechnung von Fraktionierkolonnen für Vielstoffgemische.** 50 pp. text, 36 pp. tables. Springer-Verlag Berlin, Göttingen, Heidelberg 1951. Price D.M. 18 or 31s. 6d.

It is disappointing to see that, in a recent text on fractionation, *RAOULT's law* and the thermal properties of pure substances are still used to calculate vapour-liquid equilibria and the heat of vaporization in a mixture. The author is apparently not familiar with the enormous amount of research on equilibrium constants in particular of hydrocarbons and the thermal properties of components when they occur in a mixture. In Table 15 the vapour pressures of paraffin hydrocarbons, defined by their boiling points at 1 kg/cm<sup>2</sup> abs, are represented as a function of temperature. Beyond the critical temperature of the pure component its vapour pressure has been extrapolated by the aid of a special nomogramme analogous to the Cox chart, a procedure that one would certainly not expect in a modern book on distillation. It is only on the last page of the text (p. 50) that fugacities are mentioned, when it is said that the author has not investigated whether the use of fugacities or activities instead of pressures would be of advantage since it is not possible to represent by a simple graphic method deviations from ideal behaviour in multicomponent mixtures!

The subjects treated are pressure-temperature curves, equilibria of multicomponent mixtures (dew and bubble point calculations), flash vaporization, enthalpy of vapour-liquid mixtures [the latent heat of the pure substance is used for this calculation and it is stated (p. 21) that there are no data about latent heat of a component in a mixture at temperatures higher than the critical temperature of the pure component!], calculations of distillation of binary mixtures according to MCCABE's and THIELE's method, and of multicomponent mixtures by plate to plate computation.

The book is certainly not at the level of HAUSBRAND's, THORMANN's and KIRSCHBAUM's famous monographs, but it may be used as a first introduction. The author's enthusiasm for his subject is reflected in the style in which the treatise is written. W. R. VAN WIJK